REVISTA DE LA
ASOCIACIÓN GEOLÓGICA ARGENTINA
www.geologica.org.ar

Volumen 78 (2)

Junio 2021

Stratigraphy and depositional architecture of the Viamonte Formation, Miocene, Tierra del Fuego, Argentina: the interplay between deep-marine transverse and longitudinal depositional systems

Eduardo B. OLIVERO[1,2] and Pablo J. TORRES CARBONELL[1]

[1]Laboratorio de Geología Andina, Centro Austral de Investigaciones Científicas (CADIC-CONICET), Ushuaia, Tierra del Fuego.

[2]Universidad Nacional deTierra del Fuego, ICPA, Ushuaia, Tierra del Fuego.

E-mails: emolivero@gmail.com; torrescarbonell@cadic-conicet.gob.ar

Editor: Diego A. Kietzmann

Recibido: 28 de junio de 2020

Aceptado: 27 de septiembre de 2020

ABSTRACT

Miocene, foreland Austral basin strata of the Viamonte Formation in the Atlantic coast of Tierra del Fuego are currently interpreted as deep marine channel-levee complexes. New data on sedimentary facies, paleocurrents, and stratigraphic relationships documents, however, more complex settings. We recognize in the Viamonte Formation three higher-rank architectural elements: 1) a transverse system of gullies and other slope deposits, including gully axis, gully off-axis/gully margin, and slope-gully abandonment sub-elements; 2) an axial system, the channel belt, including channel fill, lateral accretion, internal-levee/terrace, and basal slumps sub-elements; and 3) another axial system, the external levee. Gullies in the transverse system are carved into external-levee deposits of the Viamonte Formation or older lobe deposits. Dominant sedimentary facies are mass transport deposits in the gully fill; thin-bedded turbidites in the external levee, internal levee, and terraces; and thick, high-density turbidite sandstones in the channel fill. In the transverse system, paleocurrents are directed to the NW-NE, down dip high-relief progradational clinoforms, and in the axial systems to the SE, parallel to the basin foredeep. Axial systems are located either at the base, or at subtle slope-breaks of transverse clinoforms. The envisaged depositional architectures of these axial and transverse systems offer excellent analogues for similar, poorly exposed Upper Cretaceous-Paleogene Austral basin turbidites and may help to interpret the source and routing of sand-rich deposits in the adjacent Malvinas foreland basin.

Keywords: Austral/Malvinas basin, Foreland basin, Architectural elements, Channel levee complexes, Gully fill.

RESUMEN

Estratigrafía y arquitectura depositacional de la Formación Viamonte, Mioceno, Tierra del Fuego, Argentina: interacción entre sistemas depositacionales marinos profundos transversales y longitudinales .

Los depósitos miocenos de la Formación Viamonte, cuenca de antepaís Austral, costa atlántica de Tierra del Fuego, fueron interpretados como complejos de canal-albardón marinos profundos. Nuevos datos de facies sedimentarias, paleocorrientes y relaciones estratigráficas evidencian, sin embargo, paleoambientes más complejos. En este trabajo se reconocen en la Formación Viamonte tres elementos arquitecturales mayores: 1) un sistema transversal, cárcavas (gullies) y otros depósitos de talud depositacional (clinoformas), que incluye depósitos axiales, laterales/marginales y abandono de cárcava, como sub-elementos; 2) un sistema axial, faja de canales, que incluye depósitos de relleno de canal, acreción lateral, albardones internos/terrazas, y depósitos de deslizamientos basales, como sub-elementos; y 3) otro sistema axial, albardón externo. Las cárcavas del sistema transversal están incisas en albardones externos de la Formación Viamonte o en depósitos de lóbulos más antiguos. Las facies sedimentarias más comunes son depósitos de remoción en masa en el relleno de cárcavas; turbiditas delgadas en los albardones externo, interno y terrazas; y turbi-

ditas arenosas de alta densidad en el relleno de canales. Las paleocorrientes están dirigidas hacia el NO-NE, pendiente abajo de las clinoformas, en el sistema transversal y hacia el SE, paralelas a la antefosa, en el sistema axial. Los sistemas axiales se localizan en la base o en quiebres de pendiente de las clinoformas transversales. La arquitectura depositacional interpretada para estos sistemas transversales y axiales constituye un excelente análogo en depósitos turbidíticos semejantes del Cretácico Superior-Paleógeno de la Cuenca Austral y puede facilitar la interpretación del origen y dispersión sedimentaria de depósitos arenosos en la adyacente cuenca de antepaís Malvinas.

Palabras clave: Cuencas Austral/Malvinas, Cuencas de antepaís, Elementos arquitecturales, Complejos de canal-albardón, Relleno de cárcavas.

INTRODUCTION

In depositional systems of tectonically active foreland basins the interplay between transverse and axial depositional systems is critical for proper evaluation of the source, routing and location of sand-rich deposits. Foreland basins are generally characterized by complex sedimentary fill histories resulting mainly from lateral differences in tectonic load, thickness and mechanical properties of the lithosphere, and the simultaneous, combined operation of contractional tectonics and sedimentation processes (Allen and Homewood 1986, Decelles and Giles 1996). This complexity is well illustrated by the foreland Austral-Magallanes basin, which extends for more than 1000 km along the eastern, northeastern, and northern flanks of the Patagonian Andes and the Fuegian Andes (Fig. 1). On the northwestern reaches of the thrust-fold belt in Última Esperanza region, Chile, the sedimentary facies, architecture and paleogeography of the Upper Cretaceous-Paleogene depocenters are influenced by lateral variations in thickness and mechanical properties of an attenuated continental crust. The resulting foredeep was elongated in a north-south direction and flanked in the north by southward dipping clinoforms, prograding in a longitudinal (axial) direction (Romans et al. 2011, Fosdick et al. 2014, Ghiglione et al. 2014). Conversely, on the southeastern reaches of the basin in Península Mitre, easternmost Tierra del Fuego, Argentina, where the Austral basin connects with the Malvinas basin, the east-west axially elongated Upper Cretaceous-Paleogene depocenters in the thrust-fold belt were mainly sourced from several entry points through northward-directed, transverse fan-delta systems (Olivero et al. 2002, 2003, Torres Carbonell and Olivero 2019). In addition, these fan-delta systems appear to supply the clastic material to axial channel-levee systems, which ultimately were interpreted to provide clastic material to sand-prone frontal splay deposits further east, in the western Malvinas basin (Torres Carbonell and Olivero 2012, 2019). These ENE trending channel-levee systems and their interpreted associated sand-prone frontal splay deposits may explain (Torres Carbonell and Olivero 2012, 2019) a similarly oriented, thick Paleogene depocenter in the southwestern part of the Malvinas basin (Galeazzi 1998, Tassone et al. 2008, Baristeas et al. 2013).

A complete architectural reconstruction of the interaction between axial and transverse depositional systems in the Upper Cretaceous-Paleogene rocks in the thrust-fold belt of easternmost Tierra del Fuego is hampered by structural complexities (Torres Carbonell et al. 2011, 2013, 2017a, b) and limited exposures. Nevertheless, in a combined structural and stratigraphic analysis Torres Carbonell and Olivero (2019) have also studied the youngest Oligocene-Miocene depocenter located north of the thrust-fold belt front of the Austral Basin in Tierra del Fuego. Part of this youngest depocenter has been imaged in seismic lines as consisting of axial foredeep depositional systems, flanking the Rio Chico Arch on the east and of transverse, NE prograding, oblique clinoforms on the west (Fig. 1b-d, Torres Carbonell and Olivero 2019). These axial systems are located at subtle slope breaks along the strike of the transverse, NE dipping clinoforms. In particular, an integral part of this Oligocene-Miocene depocenter --the Cabo Viamonte beds of Malumián and Olivero (2006)-- has been previously interpreted as channel-levee complexes (Ponce et al. 2008, Ponce and Carmona 2011a); thus, these beds seem to offer and excellent analogue to study the interactions between axial and transverse depositional systems in the Austral basin of Tierra del Fuego. Furthermore, a more complete understanding of the interplay between axial and transverse depositional systems in the Austral basin may help to interpret the source, routing and depositional settings of sand-rich deposits in the adjacent Malvinas basin.

In preliminary, pioneering stratigraphic and sedimentological studies the Cabo Viamonte beds were interpreted as a relatively uniform package of deep-marine channel-levee turbidite complexes originated from hyperpycnal flows at the base of a depositional slope (Malumián and Olivero 2006, Ponce et al. 2008, Ponce and Carmona 2011a). In this study we present a new interpretation, with a more complete description of the stratigraphy, depositional architecture, sedimentary facies, and sedimentary dispersion of the Cabo Viamonte beds --af-

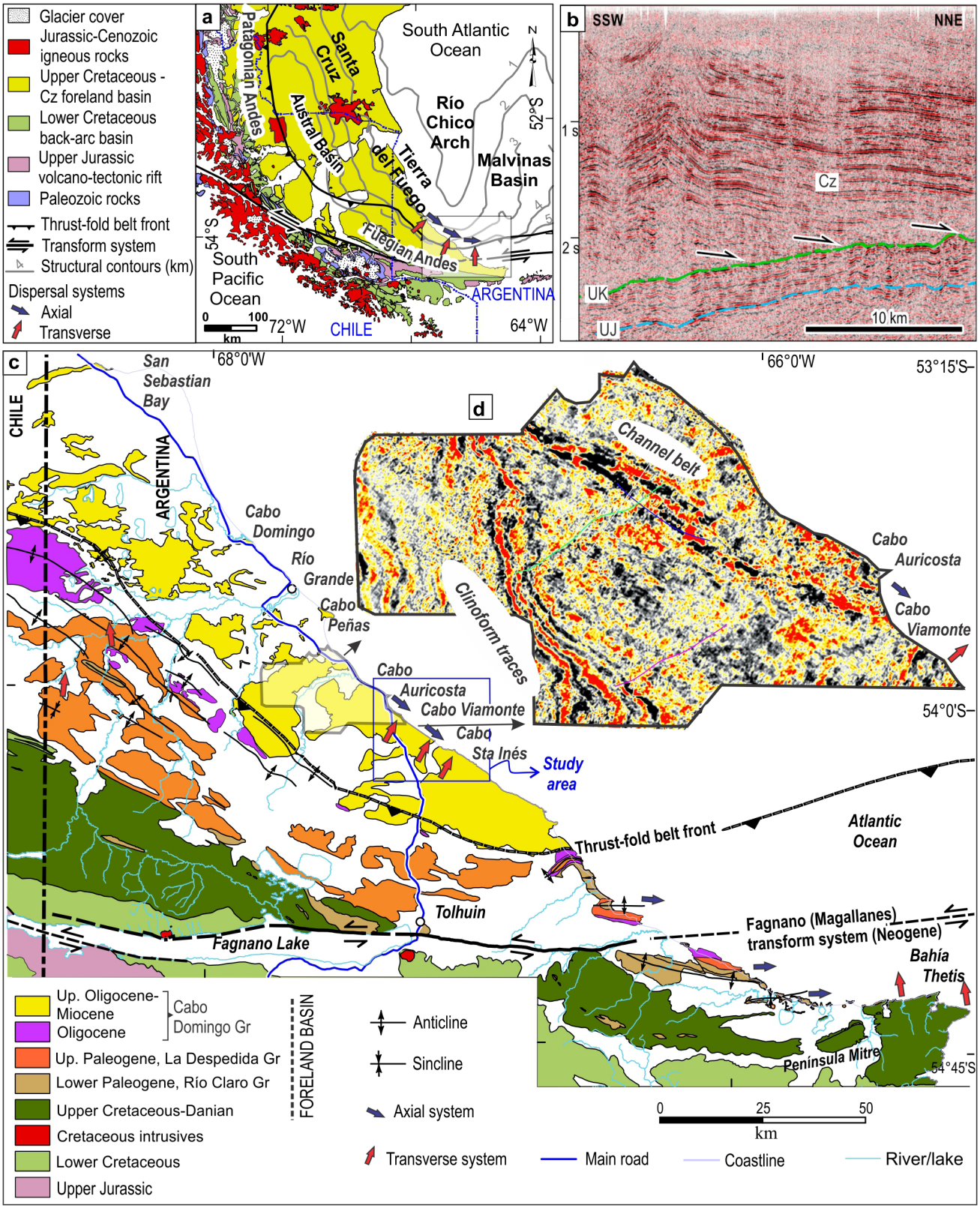

Figure 1. Geology of the Austral/Magallanes basin. a) Location and general geology; b) Seismic line showing the marked flexural subsidence, evident NE clinoform progradation, and associated foreland unconformity (arrows) of the foreland basin fill. The youngest structures of the fold-thrust belt are evident to the SSW. UJ and UK: top of Upper Jurassic and Upper Cretaceous rocks, respectively; Cz: Cenozoic rocks; c) Geological sketch of the Fuegian Andes depicting paleocurrent trends in transverse and axial systems. The shaded polygon indicates location of the inset d and the blue square the study area; d) Subsurface 3D time-slice data showing traces of clinoforms and axial channel fill complex. Modified from Torres Carbonell and Olivero (2019).

terward formalized as Viamonte Formation-- along the Atlantic coast of Tierra del Fuego, between the localities of Cabo Auricosta and Cabo Santa Inés (Fig. 1). In our study, we recognize in the Viamonte Formation three fundamentally different sedimentary packages, consisting of relatively large slope gullies (or small canyons) and other slope deposits; channel complex deposits; and external levee deposits, which in turn are subdivided into several subunits. Thus, the main objectives of this study are to interpret the stratigraphy, particularly the spatial relationships of depositional elements of the Viamonte Formation, and to model and discuss the interplay and connection between depositional systems in axial channel-levee complexes and transverse slope gullies.

GEOLOGICAL SETTING

The Austral-Magallanes foreland basin system extends along the front of the southernmost Andes from northwestern Santa Cruz (Argentina) and eastern Magallanes-Última Esperanza (Chile) to the South Atlantic Ocean (Fig. 1), where it connects with the western Malvinas basin (Biddle et al. 1986, Galeazzi 1998, Malumián 2002, McAtamney et al. 2011, Sachse et al. 2015, Malkowski et. al. 2017, Torres Carbonell and Olivero 2019). In Tierra del Fuego, Argentina (Fig. 1), the Upper Cretaceous-Cenozoic sedimentary infill of the Austral-Magallanes basin accumulated synchronously with several contractional stages that followed a major, ductile deformation phase associated with the closure and inversion of the predecessor Late Jurassic-Early Cretaceous Rocas Verdes back-arc basin (Dalziel 1981, Klepeis et al. 2010, Torres Carbonell et al. 2020, and the bibliography therein).

From the Late Cretaceous to the Oligocene-earliest Miocene, the sedimentary fill of the foreland basin system includes thick, unconformity-bounded, syntectonic clastic wedges accumulated in successive elongated foredeeps oriented subparallel to the Fuegian Andes (Fig. 1). South of the deformation front and within the thrust-fold belt, these clastic wedges are dominated by turbidite systems that include the Campanian-Danian Bahía Thetis and Policarpo formations; the Paleocene-lower Eocene Río Claro Group; the upper mid Eocene-lower Oligocene La Despedida Group; and part of the Oligocene-Miocene Cabo Domingo Group (Olivero and Malumián 1999, 2008, Olivero et al. 2002, 2003, López Cabrera et al. 2008, Martinioni 2010, Torres Carbonell 2010, Torres Carbonell et al. 2011, 2013, 2014, 2017a-b, Torres Carbonell and Olivero 2012, 2019, Bedoya-Agudelo 2019). North of the deformation front, the major part of the Cabo Domingo Group consists of subhorizontal strata (Malumián and Olivero 2006, Olivero and Malumián 2008, Ponce et al. 2008, Ponce 2009, Ponce and Carmona 2011a, Torres Carbonell and Olivero 2019).

Sedimentation of these clastic wedges was closely related to the evolution of the Fuegian thrust-fold belt and dominated by axial and transverse turbidite systems, the clastic material of which was derived from the Fuegian Andes and the South Patagonian andesitic magmatic arc (cf. Olivero 2002, Hervé et al. 2007, Barbeau et al. 2009, Torres Carbonell 2010, Torres Carbonell and Olivero 2019). Within the thrust-fold belt or close to the deformation front, tectonostratigraphic controls dominated the foreland basin sedimentary fill architecture. These controls resulted in two major depositional systems: (a) a submarine ramp formed by progradational oblique clinoforms, with transverse sedimentary dispersal, and (b) an axial depositional system developed at the base of the submarine ramp, with sedimentary dispersion along the foredeep (Torres Carbonell and Olivero 2019). Formed during orogenic growth stages, submarine ramp deposits are typified by coarse-grained, fan-delta conglomerates and sandstones (e.g. the Campanian-Maastrichtian Bahía Thetis Formation; the Paleocene Tres Amigos Formation, Río Claro Group; the Eocene Ballena Formation, La Despedida Group; and the lower Oligocene Tchat-chii Formation, basal Cabo Domingo Group) and fine-grained, muddy slope deposits and mass transport deposits (MTDs), for example the Oligocene Puesto José and Desdémona formations, Cabo Domingo Group.

Within the thrust-fold belt, the long-lived axial depositional system (b) is characterized by remarkable turbidite systems, dominantly formed by channel-levee complexes (Torres Carbonell and Olivero 2012, 2019), characteristic of the lower Eocene Punta Noguera and Punta Torcida formations, Río Claro Group and the mid-upper Eocene to lower Oligocene Cerro Colorado Formation, La Despedida Group. The long-lived channelized, axial turbidite systems were interpreted to act as an east-west conduit for sediments sourced at the Fuegian Andes and transported to a deeper depositional zone in the adjacent Malvinas Basin. Levee confinement of the channelized turbidity flows located in the foredeep transfer zone at the base of, or within oblique, progradational clinoforms suggests that the sandier portion of the flows was able to reach a depositional zone, where mostly unconfined (sheeted) sand bodies may have formed frontal splay deposits in the western Malvinas basin (Torres Carbonell and Olivero 2012).

To the north of the thrust-fold belt front (Fig. 1), the dominantly subhorizontal strata of the Cabo Domingo Group originated after cessation of the contractional deformation in the Fuegian Andes. They consist of transverse depositional systems, characterized by the development of progradation-

al-aggradational oblique clinoforms to sigmoidal, deltaic clinoforms, and axial channel-levee complexes developed at the base, or at subtle slope-breaks of the clinoforms. These strata configure a notable progradation of depositional systems from the orogenic front towards the basin center, and along the narrow SE-oriented moat inherited from the last foredeep and confined at its northeastern margin by the Rio Chico Arch topography (Torres Carbonell and Olivero 2019). The stratigraphy, depositional architecture and interconnection between Miocene, transverse slope deposits of the prograding oblique clinoforms and axial, channel-levee complexes present at slope breaks along the strike of the clinoforms are the main focus of this study.

METHODOLOGY AND TERMINOLOGY

The sedimentary rocks of the Viamonte Formation are largely exposed on vertical cliffs up to 135 m high. Consequently, in most cases only the exposed base of the cliff is accessible to detailed studies of sedimentary facies, whereas upper reaches are difficult to study, particularly regarding determination of grain-size, textures, and small-scale sedimentary structures. These difficulties were partly compensated through (1) observations in recent rock falls whose stratigraphic position could be reasonably deciphered and (2) recognition of apparent lithological similarity with beds exposed at the base of the cliff. In consequence, sedimentary facies could only be char-

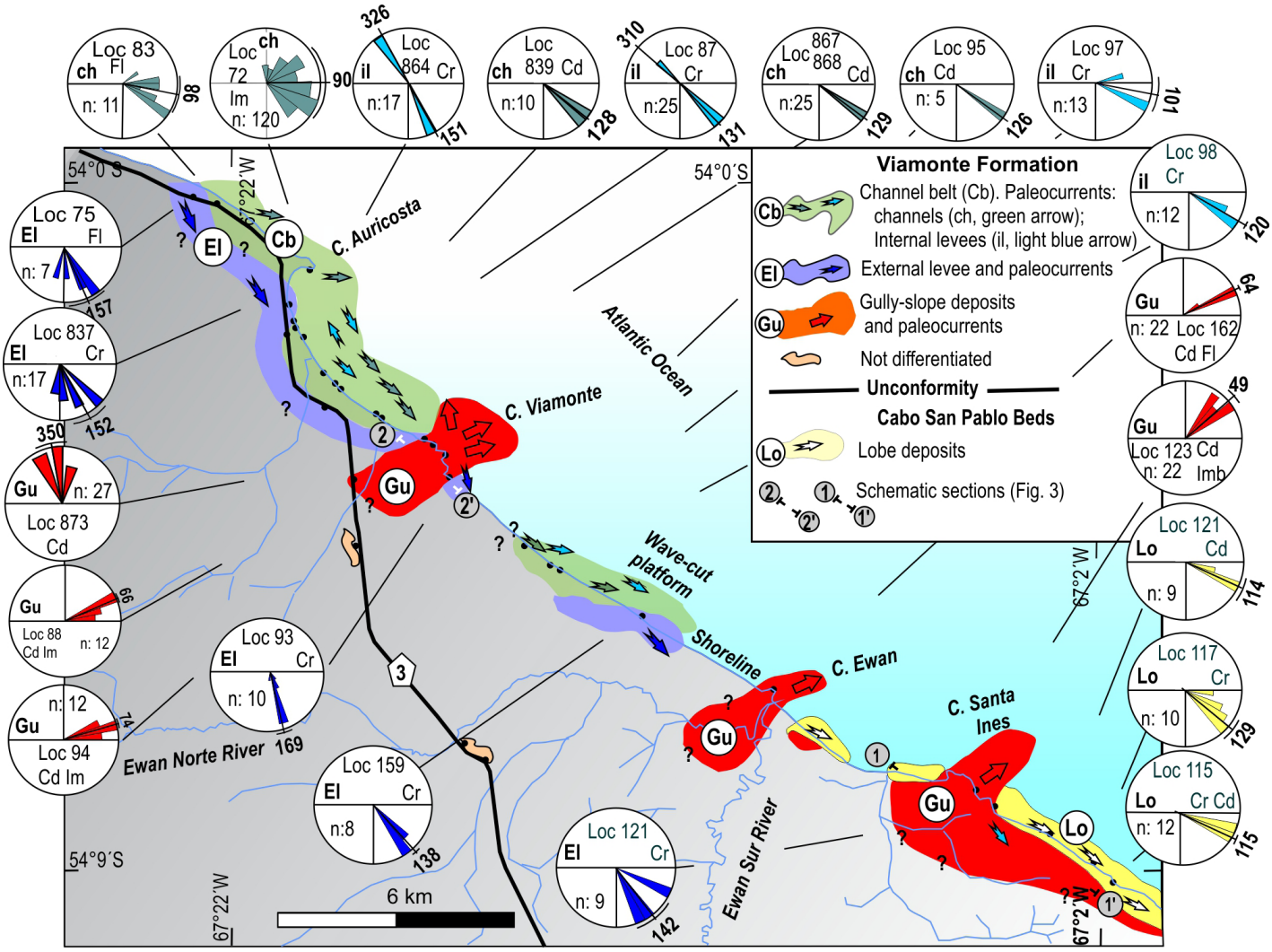

Figure 2. Geological map and paleocurrents of channel belt (Cb), with channels (ch) and internal levees (il); external levee (El); and gully fill (Gu) architectural elements of the Viamonte Formation, and depositional lobes (Lo) of the Cabo San Pablo beds. Paleocurrent vectors measured from flute casts (Fl); clast imbrication (Im); climbing ripples (Cr) and climbing dunes (Cd) at different localities (black dots, see also sections in figure 3a-b). For each rose diagram, the number of measurements (n) at a given locality (loc.) and vector mean (bold number) are shown. Large arrows: mean paleocurrent directions for different settings.

acterized at a large-scale. Conversely, the actively retreating sea cliffs offer continuously fresh rock exposures, displaying spectacular views of the internal large-scale geometrical and architectural relationships of the sedimentary packages.

For the characterization and interpretation of the deep-marine deposits and depositional settings of the Viamonte Formation we follow the approach of depositional or architectural elements (Mutti and Normak 1991), which is one of general use for characterization and comparison of turbidite systems (cf. Schwarz and Arnott 2007, Hubbard et al. 2008, Crane and Lowe 2008). As summarized by Posamentier and Walker (2006), the identification of larger-scale depositional or architectural elements made possible their linkage into depositional systems. In our study, depositional or architectural elements are defined by (1) their external geometries and (2) the internal facies within the elements. Our analysis integrates stratigraphic, geometrical, paleocurrents, and facies observations based on outcrop as well as limited seismic data (Figs. 1, 2). Deep-water depositional elements of the Viamonte Formation are of the order of tens of meters in thickness and may extend laterally for tens or hundreds of meters. In this regard, the relatively large-scale used in the characterization of depositional elements allows to minimize the problems of close observation of sedimentary facies mentioned above. The scale of our approach is equivalent to the fourth-order elements composed of genetically related lithofacies, whose bounding surfaces separate distinctive geometrical sedimentary bodies, used in a conceptually similar scheme for the Upper Cretaceous deposits in the Última Esperanza region, Chile (cf. Hubbard et al. 2008, Crane and Lowe 2008).

Due to the inherent problems of outcrops in vertical cliffs, it was not possible to measure detailed sedimentary logs. To compensate this deficiency, we constructed lateral panels integrating surface-based panoramic photographs combined with altitude and distance measuring using hand clinometer, laser range-meter and GPS location. These panels were very useful for depicting the large-scale geometrical and lateral relationships of different depositional elements (e.g. Figs. 3a-b, 4-6).

There is no general agreement on the terminology used for description of depositional systems and architectural elements in deep-marine settings. Canyons are generally conceived as large relief erosional conduits, limited by steep margins several kilometers apart and excavated several hundreds meters below the adjacent sea floor. Within the canyons, downslope moving gravity flows are considered to be wholly confined by the steep relief so that no levees are developed. Gullies are also negative relief features but of much smaller dimensions; a few tens of meters deep and hundreds of meters wide (see Posamentier and Walker 2006, Mulder 2011 and references therein). The erosional conduits described here have minimum cross-sections about 2-3 km wide and 70-100 m deep (Fig. 3a-b); thus their dimensions are closer to those ascribed to small canyons or large gullies (Mulder 2011) and for descriptive purposes we refer them as gullies in this study.

For the channel belt and associated levees we follow the terminology used by Kane and Hodgson (2011) and Hansen et al. (2015): channels with their associated levees are channel-levee systems; when a sediment body is the result of continuous migration or aggradation of a single channel, it is referred to as a channel fill; where a succession of channel fills are spatially coincident, the composite body is referred as a channel fill complex; and the region occupied by channel fills or channel fill complexes is referred to as a channel belt. Overbank sediments within the channel belt are either part of depositional terraces or internal levees occurring adjacent to the active channel. If over-spilling of sediment creates a wedge-shaped deposit it is called an internal levee whereas a flat deposit is called a depositional terrace. Wedge shaped features that confine channel belts are termed external levees and they are subdivided along the levee crest into inner external levee (part between levee crest and channel belt) and outer external levee (part between levee crest and termination of levee).

STRATIGRAPHY

The strata exposed in the area of Cabo Viamonte were differentiated from the rest of the sedimentary rocks of the Cabo Domingo Group (Malumián and Olivero 2006) as the Cabo Viamonte beds (i.e. the Viamonte Formation). The distinguishing lithological features were characteristical packages of thick-bedded, coarse-grained breccia; fine-grained conglomerate, sandstone and mudstone of marked large-scale lenticular geometries bounded by multiple, internal erosion surfaces. In addition, the Viamonte Formation bears abundant rounded fresh basaltic clasts and it is characterized by a dominant volcaniclastic petrographic mode. The volcaniclastic mode introduces a distinctive petrographic component that is only shared with the Castillo and Carmen Silva formations of the Cabo Domingo Group (Torres Carbonell and Olivero 2019). The base of the Viamonte Formation is defined by a striking, high-relief unconformity carved into the Cabo San Pablo beds (Fig. 3a).

Later on, the Cabo Viamonte beds were extended to include the strata exposed at Punta Basílica, in the southern

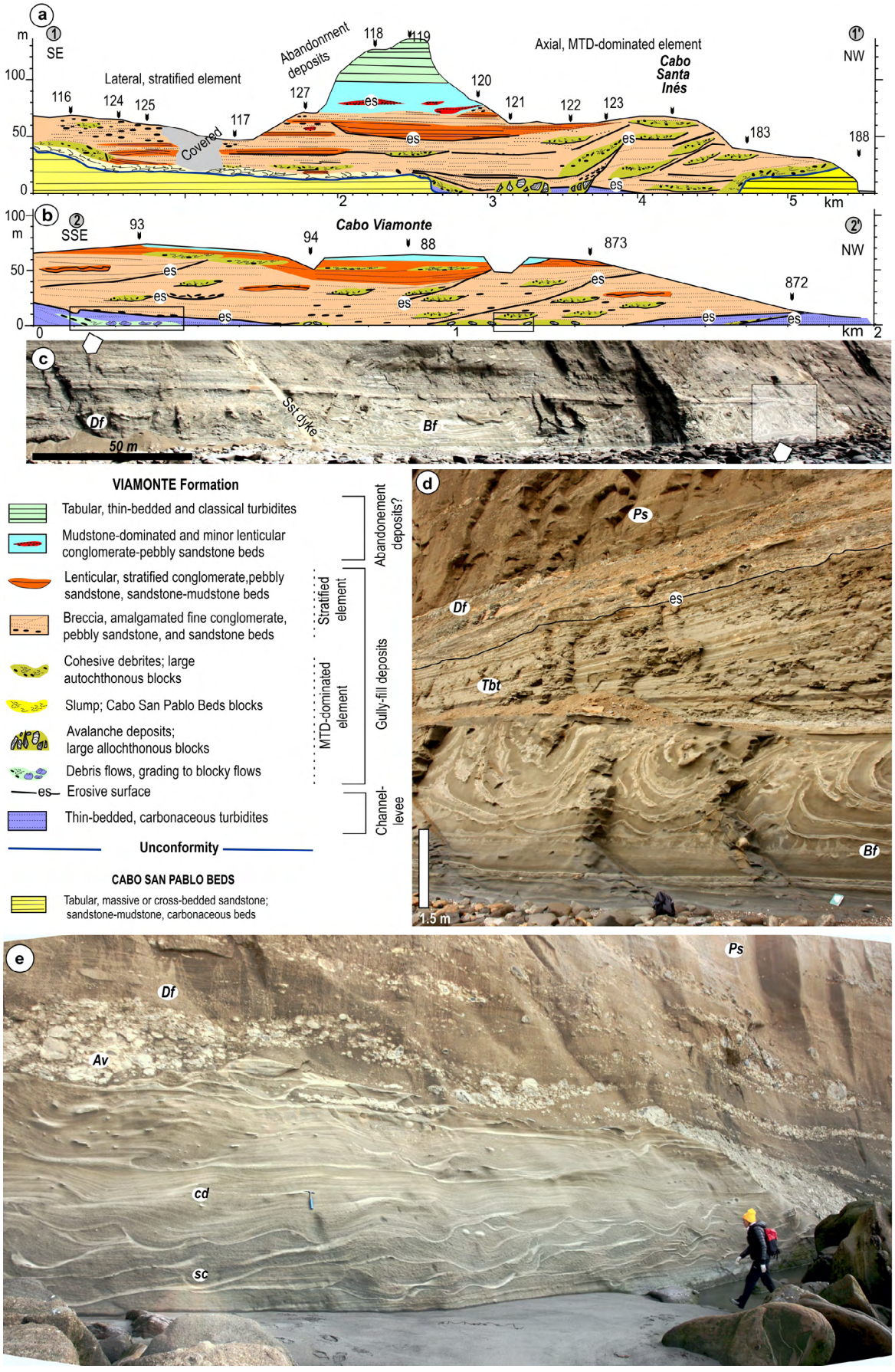

Figure 3. Gully fill and other slope deposits architectural element. a-b) Cross-sections of Cabo Santa Inés (a) and Cabo Viamonte (b) areas. The unconformity is carved into the Cabo San Pablo beds (a); at Cabo Viamonte an internal erosion surface separates the gully fill from the channel belt (b); c) Basal debris flow (Df) transitional to blocky flow (Bf) deposits; d) Detail of blocky flow deposit, thin-bedded turbidites (Tbt), and gully axis sub-element; e) Sandstone with large scours (sc) and climbing dunes (cd), covered by reworked avalanche deposits (Av). Rectangles indicate locations of C and D; (es) erosive surface; (Df) debris flow; (Ps) pebbly sandstone. Person for scale.

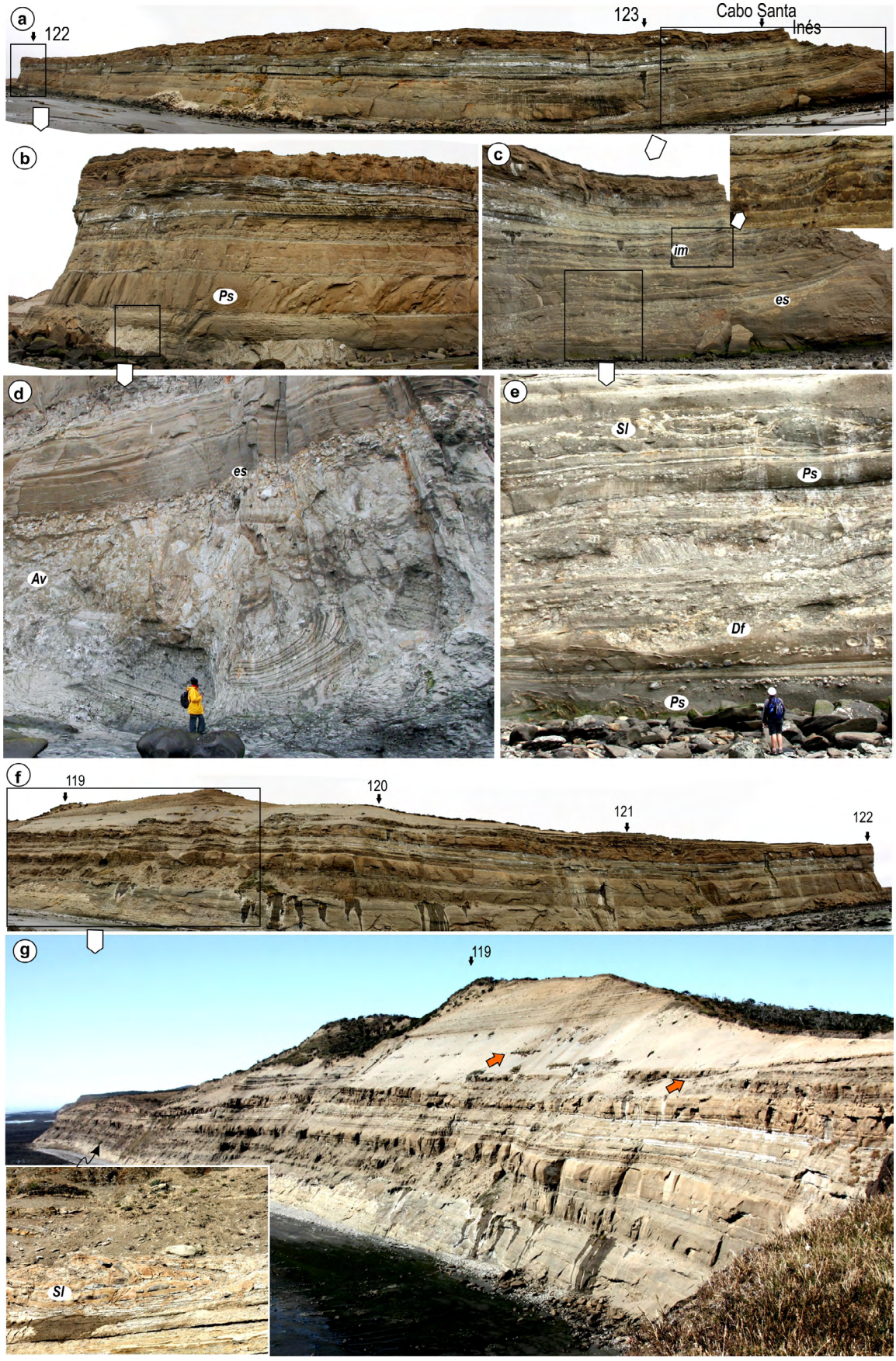

Figure 4. Gully and slope architectural element. a-e) Panoramic view of the cliff between locality 122 and Cabo Santa Inés (a) showing transition among gully off-axis (b) and gully axis (c-e) depositional sub-elements. Enlargement b shows stratified, very thick pebbly sandstone (Ps) covering debris avalanche (Av) deposit with large boulders covered by smaller cobbles at the top (D). Enlargements (c-e) show MTDs forming the cliff at Cabo Santa Inés, including large, imbricate structures (im); slump blocks with recumbent folds (sl) and cohesive debris flow deposits (df); f-g) Panoramic view of the cliff between localities 122 and 119 (f) showing transitional gully off-axis (122), gully margin (119), and gully abandonment, stratified architectural sub-elements. Gully margin and abandonment, stratified sub-elements in enlargement (g); notice channelized conglomerates in the mudstone horizon (red arrows). Close-up show the slump horizon with blocks of the Cabo San Pablo beds, just above the unconformity. For location and scale see Figure 3a.

margin of San Sebastián Bay (Fig. 1, Ponce and Carmona 2011b, Quattrocchio et al. 2018). However, the strata at Punta Basílica correspond to a different stratigraphic unit, being presently considered as an integral part of the shallow-marine, delta-influenced Carmen Silva Formation (Olivero and López Cabrera 2020). Consequently, we restrict the Viamonte Formation to cover the exposures originally defined by Malumián and Olivero (2006). Hence, the type area of the Formation corresponds to the strata cropping out at the Atlantic coast of Tierra del Fuego from Cabo Auricosta to Cabo Santa Inés. The Formation may also include the strata exposed at Cabo Domingo and Cabo Peñas, and several isolated, poorly exposed, inland mudstone-dominated outcrops, but these areas were not yet studied in detail. At the type area, the Viamonte Formation reaches a minimum thickness that varies from c. 135 m at Cabo Santa Inés to c. 75 m at Cabo Viamonte (Figs. 3, 4). Due to the marked lenticular (channelized) geometry and consequent spatial variability, a single vertical section at a particular locality cannot capture the whole lithological spectra of the formation, so the best representative type section is designated at the almost continuous cliff exposures between Cabo Santa Inés and Cabo Auricosta. Along this section, the Viamonte Formation includes two very distinctive lithological associations dominated by: (1) mass transport deposits of coarse-grained breccia, conglomerate and sandstone that are replaced laterally and upwards by better stratified graded sandstone and mudstone, and (2) lenticular, channel-shaped conglomerate, graded and massive sandstone, and bioturbated thin-bedded turbidites, commonly with abundant carbonized vegetal debris. The first lithological association is interpreted as gully fill and abandonment slope deposits and the second one as channel-levee complexes and bounding external levees (Figs. 2 and 3).

The gully fill deposits are well exposed at Cabo Santa Inés, Cabo Ewan, and Cabo Viamonte and the channel-levee complexes and external levees extend almost continuously along the Atlantic coast from Cabo Auricosta to Cabo Ewan (Fig. 2). Even though no direct evidence of stratigraphic superposition is available, we infer that the major gully fill deposits cropping out at Cabo Santa Inés and Cabo Viamonte have different stratigraphic positions, being the Cabo Santa Inés, and probably also the Cabo Ewan, exposures a little bit older than the Cabo Viamonte gully fill. This is based on the evidence that the Cabo Santa Inés strata rest directly unconformably on the Cabo San Pablo beds, whereas the strata at Cabo Viamonte erosively cut part of the channel-levee elements (Fig. 3).

The age of the Viamonte Formation is poorly constrained. Based on regional considerations Malumián and Olivero (2006) suggested a middle Miocene age. However, recent regional correlations with the Carmen Silva, Brush Lake-Filaret, and Palomares formations suggest an older age, possibly early Miocene, equivalent to other shallow marine deposits originated during the Patagonian transgression (Torres Carbonell and Olivero 2019). The finding of typical Santacrucian terrestrial vertebrate genera (*Nesodon* and *Astrapotherium*) in the younger Cullen Formation (Olivero et al. 2015, Bargo et al. 2018) and the common occurrence of typical Patagonian marine invertebrates, such as the gastropod *Perissodonta* (*ex Struthiolarella*) *ameghinoi* (Ihering) in the Carmen Silva and Viamonte formations (López Cabrera and Olivero 2018) support the interpretation of an early Miocene age for the Viamonte Formation.

The Cabo San Pablo beds (Malumián and Olivero 2006) were not studied in the present work, but both the architecture and lithology of these beds markedly differ from that of the Viamonte Formation. In the Cabo Santa Inés area, the Cabo San Pablo beds are characterized by tabular strata, composed dominantly of sandstone with minor mudstone, which were interpreted as deep-marine frontal splay (lobe) deposits (Ponce et al. 2008, Ponce and Carmona 2011b), originated below the carbonate compensation depth (Malumián and Olivero 2006).

VIAMONTE FORMATION: ARCHITECTURAL ELEMENTS

Based on scale, external geometry, and dominant lithologies the architectural elements recognized in the Viamonte Formation are grouped into three higher-rank categories that in some cases are subdivided into lower-rank components: (1) gullies and other slope deposits, which include 1.1) gully axis, 1.2) gully off-axis/gully margin, and 1.3) slope-gully abandonment sub-elements; (2) channel belt architectural element, which includes 2.1) channel fill, 2.2) lateral accretion deposits (LADs), 2.3) internal-levee and terrace, and 2.4) basal slumps sub-elements; and (3) external levee architectural element. The areal distribution of higher-rank architectural elements and their associated paleocurrents are shown in Figure 2.

Gullies and other slope deposits

For more than 6 km along the Atlantic coast, the basal unconformity of the Viamonte Formation displays a notable irregular relief in excess of 40 m carved into the San Pablo beds (Fig. 3a). On this irregular relief, three lithologically distinctive depositional sub-elements are recognized, each one characterizing different morphologies and presenting different

architectures: 1.1) gully axis, restricted to the deepest carved area of the gully; 1.2) gully off-axis to gully margin, present on areas adjacent to and of higher topographies than the former; and 1.3) slope-gully abandonment, better preserved at the highest relief of the studied area. In general, gully axis and gully off-axis/gully margin sub-elements have transitional boundaries but strongly differ in the degree of bed amalgamation (Figs. 3a; 4a-e), whereas the slope-gully abandonment sub-element has a more abrupt basal boundary and best defined, relatively continuous thin bed alternations (Fig. 4f-g).

Gully axis sub-element - mainly mass-transport deposits (MTDs): At localities 119 and 183 the basal unconformity delineates convergent, steeply inclined surfaces pointing towards the axis of the Cabo Santa Inés gully (Fig. 3a). A similar morphology is observed at Cabo Viamonte (Fig. 3b), but here the basal erosive surface was carved into the external levee and channel belt elements. The gully axis depositional sub-element is dominated by coarse-grained, lenticular MTDs that consist dominantly of debris avalanche deposits; debris flow and associated blocky flow deposits; slump deposits; and cohesive debrites. The base of these deposits is generally an erosive surface, with irregular channel-shaped geometry elaborated into massive coarse-grained pebbly sandstone (Figs. 3, 4), or occasionally into cross-stratified sandstone (Fig. 3e). The sedimentary facies of this architectural sub-element are essentially the same of those included within the Facies Associations 1 and partly 2 of Ponce and Carmona (2011a).

At the base of the cliff in locality 122, an impressive debris avalanche deposit is exposed with a minimum thickness of 6.5-7 m. It has a lenticular cross-section and consists of large boulders, up to 3.5 m in diameter, with scarce matrix. The top has a characteristic finer grained horizon with cobbles and small boulders, 0.2-0.5 m in diameter (Fig. 4a-d). Its monomictic lithology consists of whitish light-gray sedimentary clasts, characterized by regularly alternating mudstone and siltstone thin beds. This lithology is not known in the study area, but the boulders and cobbles were probably derived from basinal rocks, as they are quite common in other Miocene resedimented deposits. The NW margin of the avalanche deposit erosively cuts thin-bedded turbidites with abundant carbonaceous debris and climbing ripple cross-lamination. Between localities 119-120 and 123-Cabo Santa Inés, this particular horizon of thin-bedded turbidites crops out discontinuously above the basal unconformity of the gully axis sub-element (Fig. 3a). Other debris avalanche deposits, also dominantly composed of similar monomictic small boulders of light colored laminated siltstone-mudstone beds, are recorded at several places at the deepest carved part of the gullies. In several places these debris avalanche deposits were reworked by high-density gravity flows (Fig. 3e), as previously interpreted by Ponce and Carmona (2011a). Imbricated cobbles and small boulders in these reworked debris avalanche deposits indicate NNW- to NE-directed paleocurrents (localities 123; 873; 88; 94; Fig. 2). Cohesive debris flow deposits with a mix of cobbles to small boulders, dominantly composed of local concretions, and subordinated, extrabasinal rocks floating in an abundant muddy matrix are the dominant lithology in this sub-element. Associated slump deposits that incorporate deformed local blocks with recumbent folds, or faulted and folded slide blocks forming large imbricate structures are very common, comprising most of the thickness (up to 65-70 m) in the axial part of the gully (Fig. 4a, c, e). In occasions, cohesive debrites are transitional to outstanding blocky flow deposits (cf. Festa et al. 2016, Piazza and Tinterri 2020) that carry over-sized glide blocks of deformed thin-bedded carbonaceous turbidites, detached from the basal succession. Furthermore, similar thin-bedded carbonaceous turbidites cover the blocky flow deposit, lapping markedly onto its upper surface (Fig. 3b-d).

Cross-stratified coarse-grained sandstone and pebbly sandstone are occasionally present in this sub-element. They include two main facies types. One is characterized by large-scale climbing dunes and associated large-scale scours, similar to flute casts (e.g. Fig. 3e). Paleocurrent vectors measured from both structures indicate paleoflows directed to the NNE and NNW (Localities 88; 94; 123; 162; Fig. 2). The second cross-bedded facies is characterized by pebbly sandstone, breccia, and pebble conglomerate beds that fill relatively large scours, about 10 m in length, with their steeper slope consistently dipping up-current, i.e. to the SW. This is corroborated by climbing dunes and flute casts in nearby beds, which indicate paleocurrents flowing downslope, i.e. to the NE (locality 162; Fig. 2), and also by the original bedding attitude dipping to the NE (Fig. 5). These large-scale cross-bedded facies made of upslope dipping strata (backset stratification) are interpreted as cyclic steps, which are relatively large bedforms associated with series of steps marked by supercritical flow down the lee side and subcritical flow on the stoss side, separated by upslope migrating hydraulic jumps in the intervening troughs (cf. Postma and Cartigny 2014, Postma et al. 2014).

Gully off-axis/gully margin sub-element - mainly stratified deposits: For most of the studied section at Cabo Santa Inés, where this sub-element is best exposed its base appears above the 10-15 m level on the vertical cliff (Fig. 3a). Consequently, detailed and direct observations on sedimentary facies were not possible, hindering the differentiation of

gully off-axis and gully margin facies, for which reason they are conveniently lumped together. Moving away from the gully axis, the very coarse-grained lenticular and "chaotic" MTDs are laterally replaced first by amalgamated, more tabular and very thick pebble conglomerate, pebbly sandstone, and sandstone beds that become increasingly better stratified and of reduced thickness. Then, in a distal position from the gully axis these beds split into interbedding sandstone and mudstone couples. This is clearly seen in the section (Fig. 3a-b) and panoramic photographs (Fig. 4), particularly looking from locality 122 to the gully axis at Cabo Santa Inés (Fig. 4a) and away from the gully axis to locality 119 (Fig. 4f). Lenticular cohesive debrites occur intercalated at different stratigraphic levels but these are not as common as in the gully axis sub-element. The sedimentary facies of this architectural sub-element are essentially the same as those included within the Facies Associations 2 and partly 3 of Ponce and Carmona (2011a).

Even though it is not possible to study in detail the facies transition from gully off-axis to gully margins, this transition is apparent in the panoramic photographs, marked by the change from relatively amalgamated thick sandstone and pebbly sandstone beds (e.g. at locality 122, Figs. 3a, 4a) that progressively split into interstratified, relatively thinner beds of sandstones and mudstones (Fig. 4f, g). As studied in recent rock falls derived from the mid-upper levels of the cliff, fine-grained conglomerates forming part of the gully off-axis/gully margin sub-elements have a dense concentration of rounded, mudstone pebble intraclasts and allochthonous slates, metarhyolites, quartz veins and vesicular basaltic pebbles. Various invertebrate fossils, including gastropods, bivalves, corals, crustacean, crabs and balanids, are commonly found in these conglomerates.

Just above the basal unconformity of the Viamonte Formation, a highly distinctive slide-slump deposit marks a notable lithological contrast with the rest of the gully off-axis/gully margin sub-element. The slump deposit extends almost continuously for more than 2.5 km in the Cabo Santa Inés section (Fig. 3a). It has a maximum thickness of about 3-4 m and is almost exclusively composed of an internally folded slide mass and large deformed detached blocks forming a breccia, with all large blocks derived from the underlying Cabo San Pablo beds (Fig. 4g). The upper part of this slide-slump horizon is covered discontinuously by patches of cohesive debrites with a mixture of autochthonous concretions and mudstone, and allochthonous cobbles and small boulders floating in an abundant muddy matrix. The relationship of this slump deposit with the rest of the gully off-axis/gully margin sub-element is not clear. The location of the slump deposit just above the unconformity, as well as its local lithological composition, suggest an origin related to large submarine landslides affecting mainly the not yet lithified Cabo San Pablo beds. Because MTDs of the gully axis cut this basal slump deposit (Fig. 3a), we interpret that the causal landslides, promoted by the high-relief topography of the unconformity, occurred before the carving of the deepest relief that accommodates the gully axis MTDs.

Slope-gully abandonment sub-element - sandy turbidites and mudstones: The upper part of the highest gully exposures at Cabo Santa Inés and Cabo Viamonte are characterized by packages of fine interbeds of sandstone-mudstone and mudstones. Even though the strata characterizing this sub-element are inaccessible, it can be observed that the whole section in both areas is distinguished by a notable fining- and thinning-upward trend (Figs. 3a-b; 4f, g; 5d). The lithological regularity of these strata is nevertheless interrupted by occasional minor channels filled with conglomerate and coarse-grained sandstone beds (Fig. 4f-g) and rare slump horizons. The sedimentary facies of this architectural sub-element are partly the same of the Facies Association 3 of Ponce and Carmona (2011a).

Channel belt

The channel belt architectural element is superbly and almost continuously exposed along the Atlantic coast from Cabo Auricosta to Cabo Ewan (Figs. 2, 6). In the c. 2.1 km long cliffs located just NW of Cabo Viamonte it was possible to distinguish more than 14 individual channels or different segments of the same meandering channel (Fig. 6). Since the cliff is subparallel to the main paleocurrent direction, the lenticular section displayed by individual channels is in most cases subparallel-slightly oblique to the channel axis. Nonetheless, a few cases display more transverse cross-sections, e.g. channel 7n in figure 6.

Along the Cabo Auricosta-Cabo Ewan coastal sector, the multistory channel fill complex within the channel belt includes three main architectural sub-elements: (1) lenticular channel fill; (2) lateral accretion deposits (LADs); and (3) terraces and internal levees. The sedimentary facies of these architectural sub-elements are essentially the same to those included within the Facies Associations 2 and 3 of Ponce and Carmona (2011a).

In addition, the base of the channel belt lies on a poorly exposed, but highly distinctive deposit made of large, muddy slump blocks. The reduced thickness and patchy distribution of this deposit (Figs. 6a, 7a), however, prevent to make a clear classification and for ease of description this slump deposit is

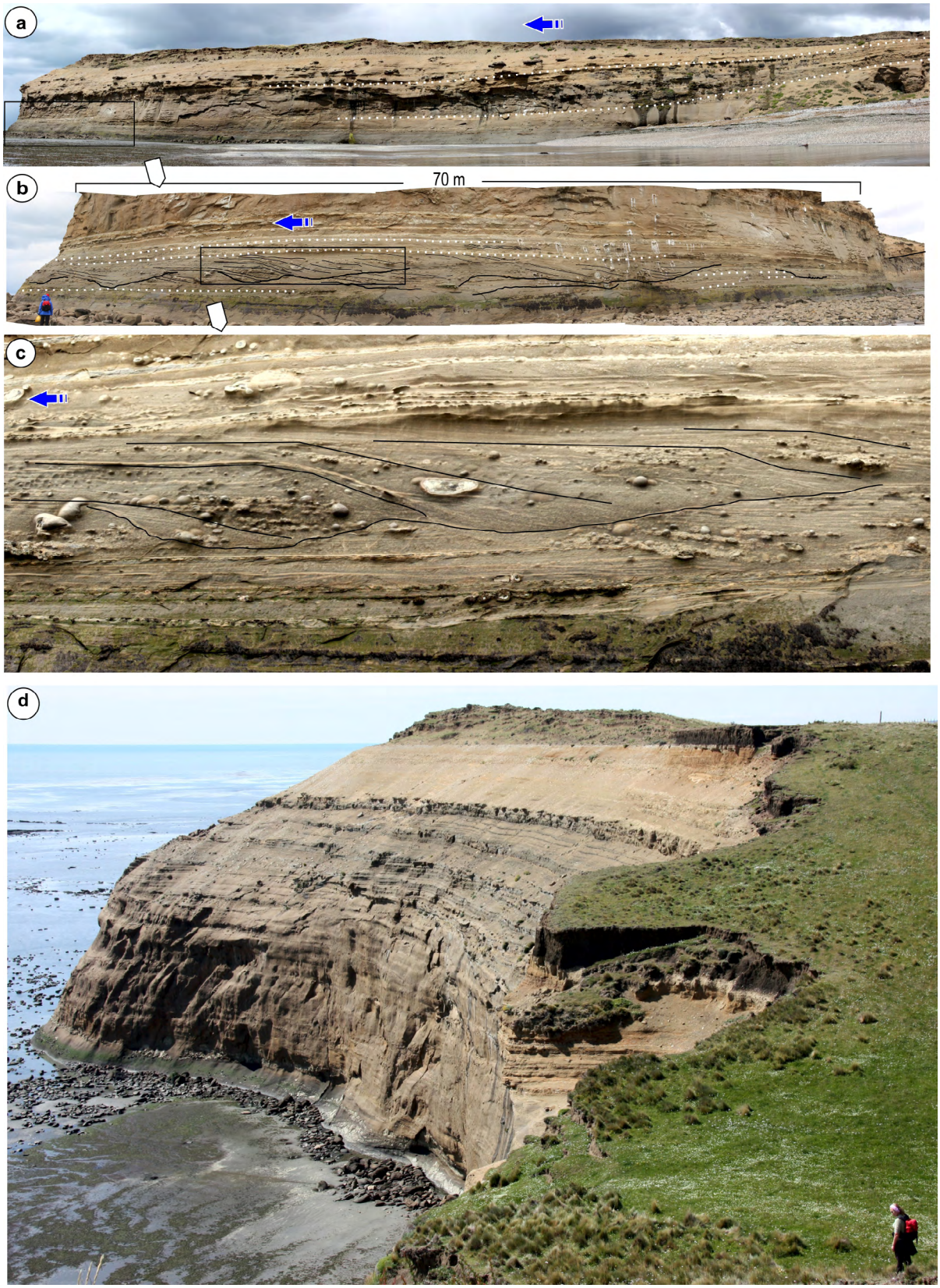

Figure 5. Gully axis and abandonment architectural sub-elements. a-c) Backset, cross-bedded strata in gully axis near Cabo Ewan; panoramic view (a) with location of large backsets (rectangle) and their relationship to the NE (left) dipping strata (white dot lines); enlargements (b, c) show details of backsets. Paleoflow (blue arrows) to the NE (left); d) Coarse-grained deposits of the gully fill covered by well-stratified turbidites and mudstone of the abandonment architectural sub-element at Cabo Viamonte (locality 88). Height of cliff c. 65 m, see section in figure 3a.

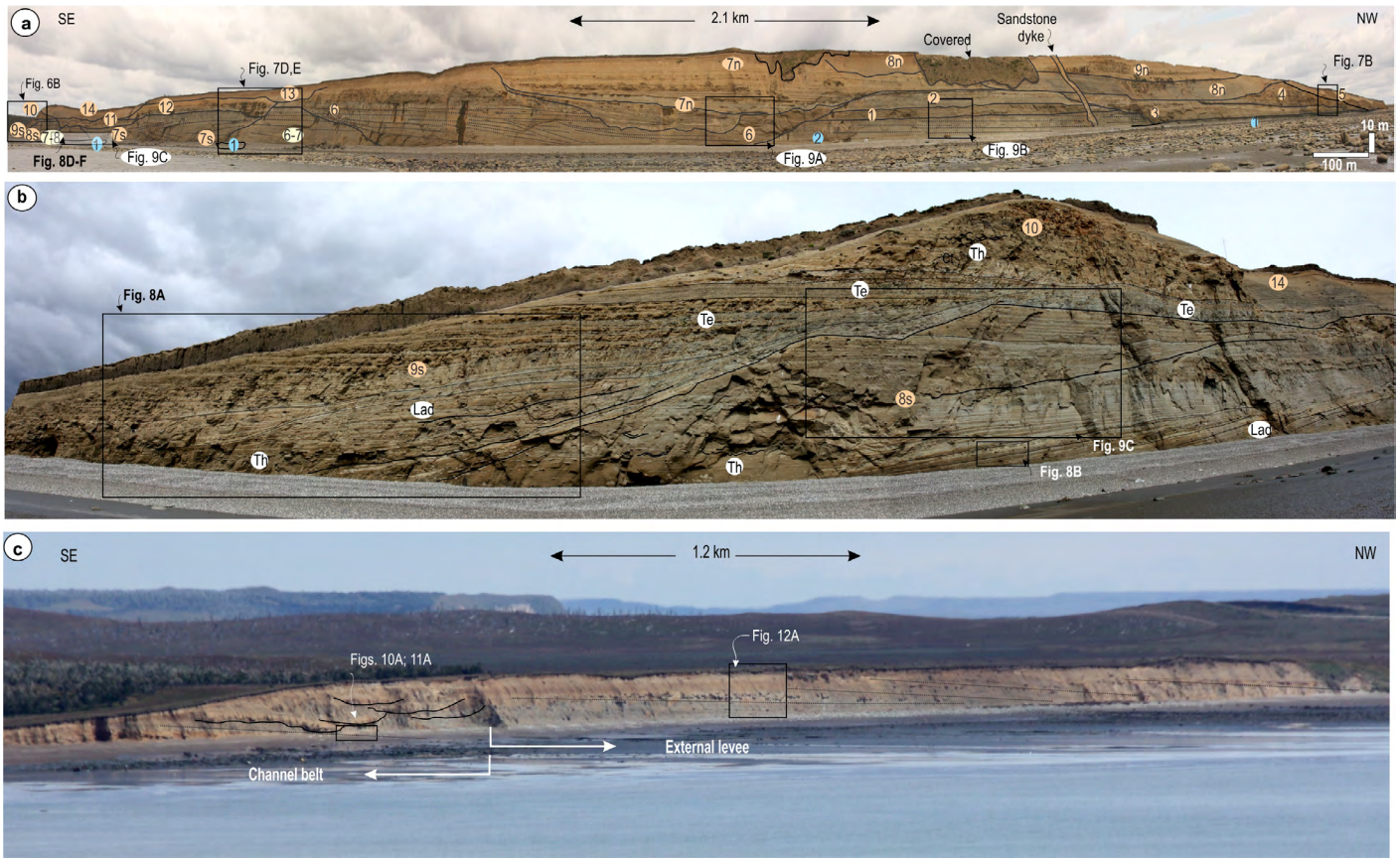

Figure 6: Channel belt and external levee architectural elements. a-b) Panoramic view (a) and detail (b) of channel belt architectural sub-elements NW of Cape Viamonte. Light blue: 1, basal slump; 2, internal levee; orange: 1 to 14, channel fill deposits of different channels or different migration stages of a single channel. Stratigraphic order of northern (7n, 8n, etc) and southern (7s, 8s, etc) channels is not always discernible. Lateral accretion deposits (Lad); channel thalweg (Th); and terrace deposits (Te); c) Panoramic view depicting relationships between channel belt and external levee architectural elements SE of Cabo Auricosta. Shaded rectangles show location of labelled figures. Notice that the external levee dips to the WSW, but the cliff exposes an apparent NW dip.

included within this channel belt as a fourth sub-element, but it may well be part of a previous channel belt system.

Lenticular channel fill sub-element - conglomerate, breccia, sandstone, and mudstone: The main features of this architectural sub-element are the characteristical fining- and thinning-upward trends of relatively thick, lenticular sedimentary successions bounded by marked, basal concave upward erosive surfaces. The succession is generally characterized by basal packages of intraclast breccia or conglomerate and thick massive or stratified pebble conglomerate and pebbly sandstone, laterally and/or vertically transitional to thick cross-bedded sandstone. Less commonly, the basal succession starts with thick, cohesive debris flow deposits. These coarse-grained facies grade upwards to interbedded, sandy turbidite and mudstone. In addition, this lenticular channel fill architectural sub-element is generally closely associated with other channel-related architectural sub-elements, such as lateral accretion deposits (LADs), terrace and internal levee deposits. Each channel-form of this architectural sub-element presents widths of about 500 m and thicknesses of 30-40 m (Figs. 7-9, 10a, 11a). The channels juxtapose laterally or stack vertically, defining in places (e.g. Fig. 6a) more than 14 different channels or different segments of the same channel.

Breccias of the basal succession are almost exclusively formed by cobbles and boulders (0.2-0.6 m) of thin-bedded mud-rich turbidites, similar to that of internal-levees and terrace deposits, into which the basal erosive surface was carved (Fig. 9a). Less common are thick cohesive debrites with meter-size boulders of autochthonous thin-bedded turbidite, mudstone and sandy concretions floating in a muddy matrix (Figs. 9c, 10a, 11a). Associated massive or stratified conglomerate and pebbly sandstone have in general a lenticular geometry, with multiple erosion surfaces (Fig. 7d-e); the largest clasts are pebble and cobble, muddy and concretionary intraclasts. In the stratified succession, intraclasts are generally aligned along distinct horizons parallel to the stratification or as lenticular accumulations of reduced thickness. Intraclast imbrication in the aligned horizons is relatively common. The matrix is a coarse-grained granule sandstone; the granules and pebbles are dominated by allochthonous clasts

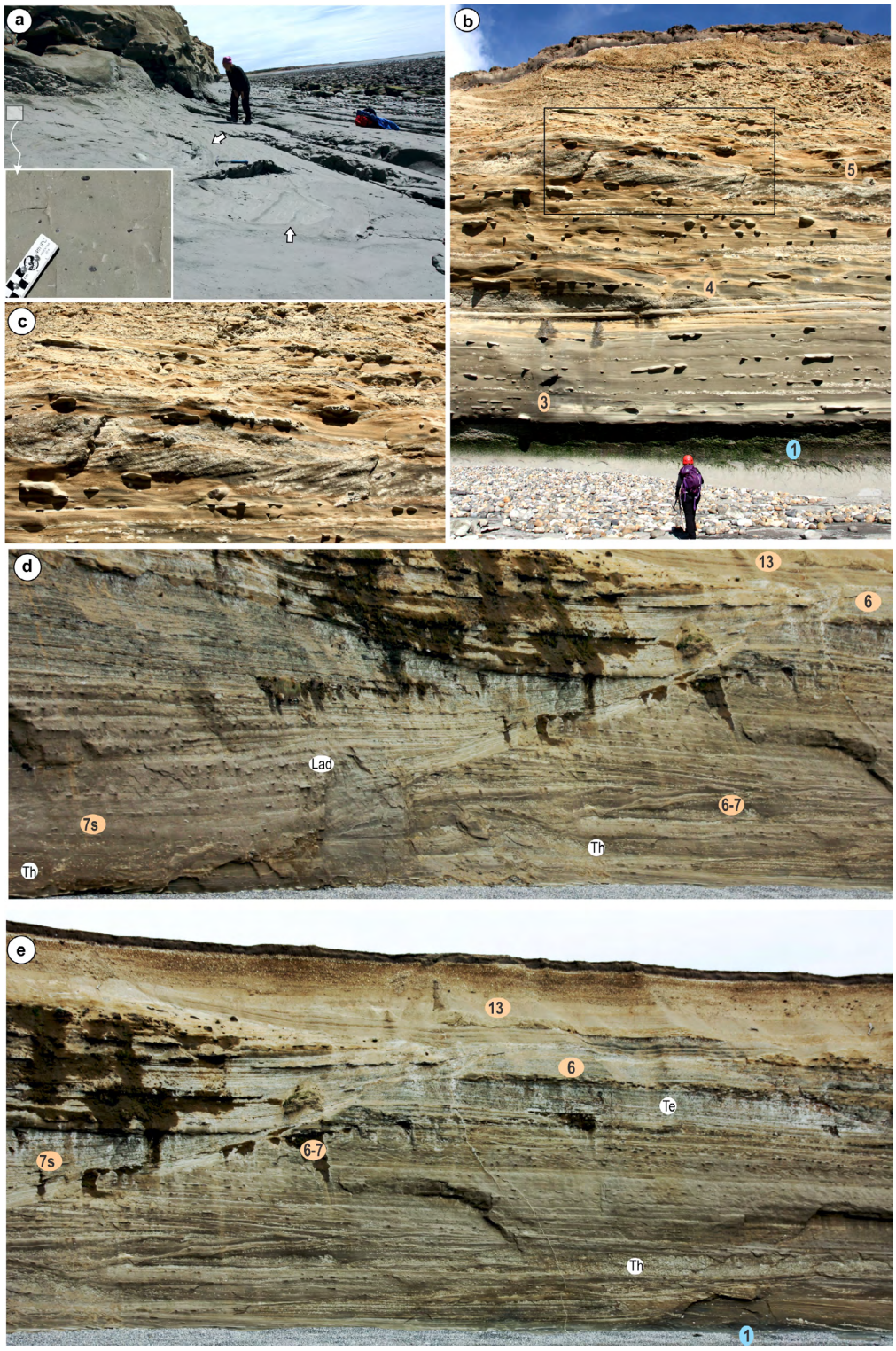

Figure 7: Channel belt architectural elements. a) Basal slump architectural sub-element, with large heterolithic blocks (white arrows) and cohesive debrites (inset). Person for scale; b-c) Coarse-grained channel fill (channels 3, 4, 5) covering the basal slump (1). Notice the cross-stratified pebbly sandstone, with backsets seemingly climbing up dip, details in inset (c) at the base of channel 5; d-e) Multiple lenticular channel fills and erosion surfaces in the thalweg (Th) of cannel 6-7 (channel number in orange circles). Other channel belt architectural sub-elements include: lateral accretion deposit (Lad), channel 7s (d) and terrace deposit above channel 6-7 (e). Notice fining-upward channel fill trend in channels 5 (b) and 13 (e). Person for scale, see also Figure 6a.

of quartz veins, slate and metarhyolite. Dewatering structures, such as pipes, dishes, and distorted beds, including large flames in occasional siltstone interbeds are common. Rarely, tabular cross-bedding and dunes are present, with foresets dipping parallel to the main flow (Figs. 8e, 9b-c) or backsets, apparently oriented in the opposite direction, climbing up dip the basal erosion surface (Fig. 7b-c).

These coarse facies grade laterally or vertically to cross-bedded pebbly sandstone and coarse-grained sandstone that display spectacular trains of climbing dunes, large flute casts, and cut-and-fill structures (Figs. 8d-f, 9a). Paleocurrent vectors measured from climbing dunes, clast imbri-

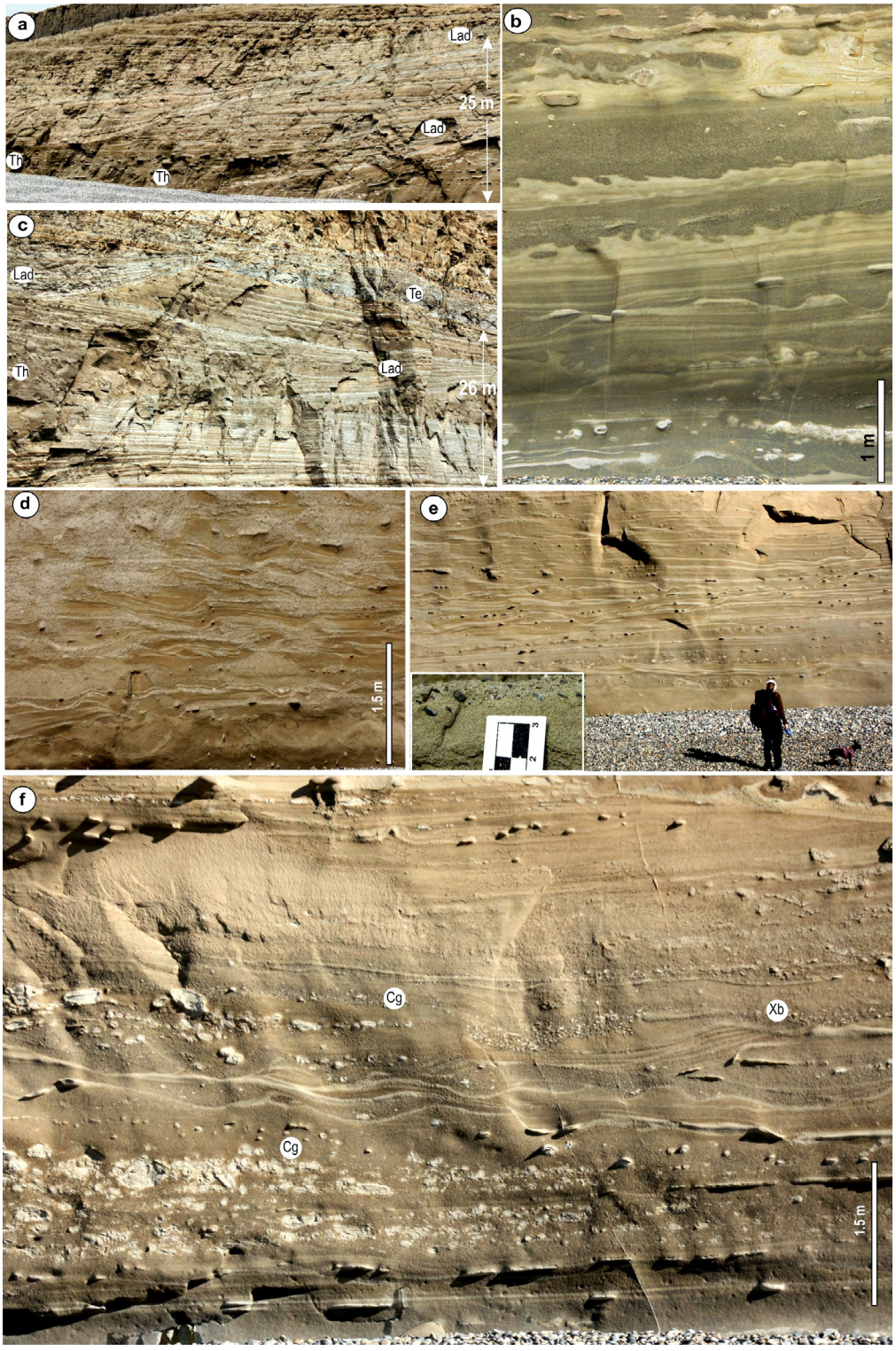

Figure 8: Channel belt architectural element. a-c) Lateral accretion (Lad) and terrace (Te) depositional sub-elements. Notice interfingering of inclined and thalweg strata in Lad, the flat surface beneath terrace deposit at upper part of channel (a, b), and large flames (c); d-f) Tractive structures in channel fill conglomerates (Cg), preserving large climbing dunes (d-e), clast imbrication (inset in e), and alternations of tabular cross-bedding strata (Xb) with aligned pebbles, cobbles and small boulders in well-defined levels (f).

cation, and flute casts indicate consistently SE-directed paleoflows (Fig. 2). The upper part of the channel fill is noticeably fine-grained, consisting of well stratified, relatively thin beds of interbedded sandstone and mudstone, and thick mudstone horizons. Most of these strata, however, are not accessible to direct inspection and only this broad characterization can be made. Nevertheless, this fining-upward trend is clearly discernible in most of the channels in the upper part of the cliff near Cabo Viamonte, particularly in channels 14, 13, 12, 9n, 8n, 7n, 6, and 5 (Figs. 6, 7e).

Lateral accretion deposits (LADs) sub-element - sandstone and mudstone: At the margin of several channels

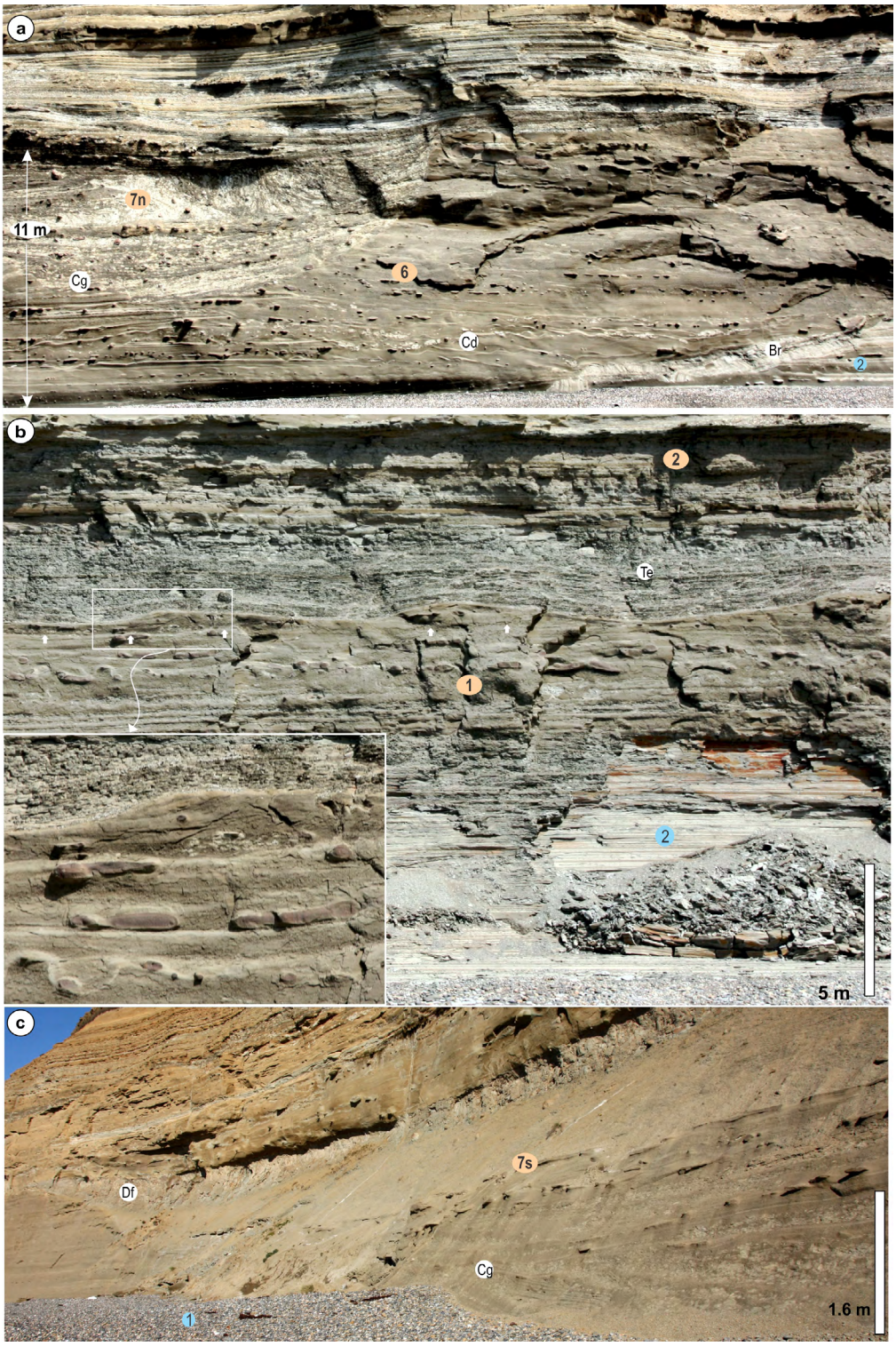

Figure 9: Channel belt architectural element. a) Breccia (Br) with autochthonous clasts eroded from the internal levee (2), sandstone with scours and climbing dunes (Cd) and conglomerate (Cg), base of channels 6 and 7n (See Figure 6a for location); b) Terrace (Te) deposits with large, basal dunes between channels 1 and 2. The base of dunes is an erosive surface (white arrows); c) Lenticular debris flow (Df) and multiple lenticular cross-bedded conglomerate (Cg) and breccia at the base of channel 7s. Pebbles and cobbles of cross-bedded conglomerate derived from the basal slump architectural sub-element (1), which in the photo is almost totally covered by a veneer of recent gravels.

there are remarkable inclined deposits that dip laterally away from the channel margin and consist of two main sedimentary facies: a lower, massive, pebble to cobble intraclast conglomerate or breccia deposit and associated coarse-grained sandstone and pebbly sandstone that grade upward, along the inclined stratification, to an upper rhythmic interbedding of progressively thinning sandstone-mudstone and mudstone turbidites (Figs. 6b, 7d, 8a-c). The lower, coarsest part is generally up to 10 m thick and the upper, rhythmical part is about 3 m thick. The inclined surfaces dip 5-11° toward the channel axis and are about 100 m long.

The lower massive conglomerate and pebbly sandstone

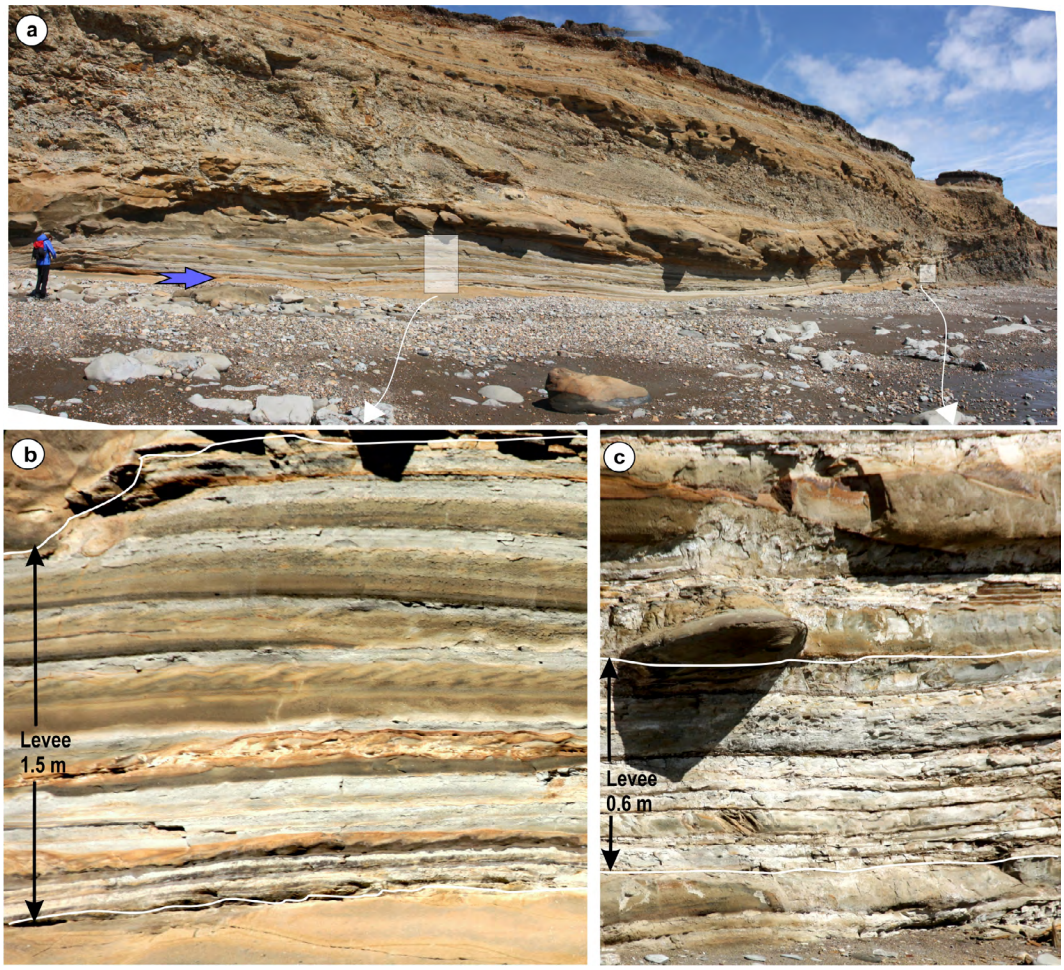

Figure 10: Internal levee architectural sub-element. a-c) Wedge-shaped internal levee and associated channels (See figure 11). Notice the change of sedimentary facies between proximal (b) and distal (c) areas in a very short distance. Turbidites with complete Bouma divisions and well-developed climbing ripples in Tc (b) are replaced by base-missing, muddy turbidites (c) in a distance of about 60 m. Paleoflow indicated by blue arrow.

form amalgamated, thick high-density turbidites that rest just above the erosive channel base and consist of the same sedimentary facies than the channel fill architectural sub-element described above. Obliquely upward along the inclined surface, these coarse-grained facies either interfinger with or are separated from progressively thinner, rhythmical turbidites by irregular erosive surfaces. Turbidites consist of thick, graded granule conglomerate-coarse-grained sandstone that thin progressively upwards to graded and laminated sandstone-mudstone turbidites. The latter bear outstanding flame structures (Fig. 8b) in the mudstone divisions and occasional traction structures (dunes) in the sandstone division. At the uppermost part of the channel-margin the rhythmical inclined turbidites are usually replaced by flat, tabular mud-rich terrace deposits (Figs. 6b, 8c). The sedimentary facies and geometry shown by the strata of this architectural sub-element are very similar, both in scale and architecture, to the lateral accretion deposits described by Schwarz and Arnott (2007) and Arnott (2007) for the Neoproterozoic Isaac Formation, Canada.

Terraces and internal levees sub-element - thin-bedded turbidites and mudstone: At the upper marginal part of the channel fill architectural sub-element there are several highly distinctive sedimentary packages dominated by thin-bedded turbidites. In most of the cases they are exposed on the inaccessible, upper cliff sectors and cannot be inspected directly; a few of them, however, are accessible to close observation. Besides their location at the upper margin of a channel system, they are characterized by a variety of sandy and muddy thin-bedded turbidite facies displaying two distinctive geometries, conforming either tabular (Figs. 6b, 7e, 8c, 9b, 11a) or wedge-shaped sedimentary bodies (Figs. 9b, 10, 11). Since it is not always possible to recognize the diagnostic geometry (Kane and Hodgson 2011, Hansen et al. 2015), they are lumped together in one architectural sub-element, representing either terraces or internal levees.

Well-exposed internal levees have wedge-shaped cross-sections, ranging between 500-100 m in length and 10-2 m in thickness. Their highly distinctive sedimentary facies are characterized by a marked variability, both in terms of distribution of Bouma divisions and paleocurrents. Close to the channel margin they consist of relatively thick (up to 0.25-0.30 m) turbidites with complete T*abcd* Bouma divisions (Fig.

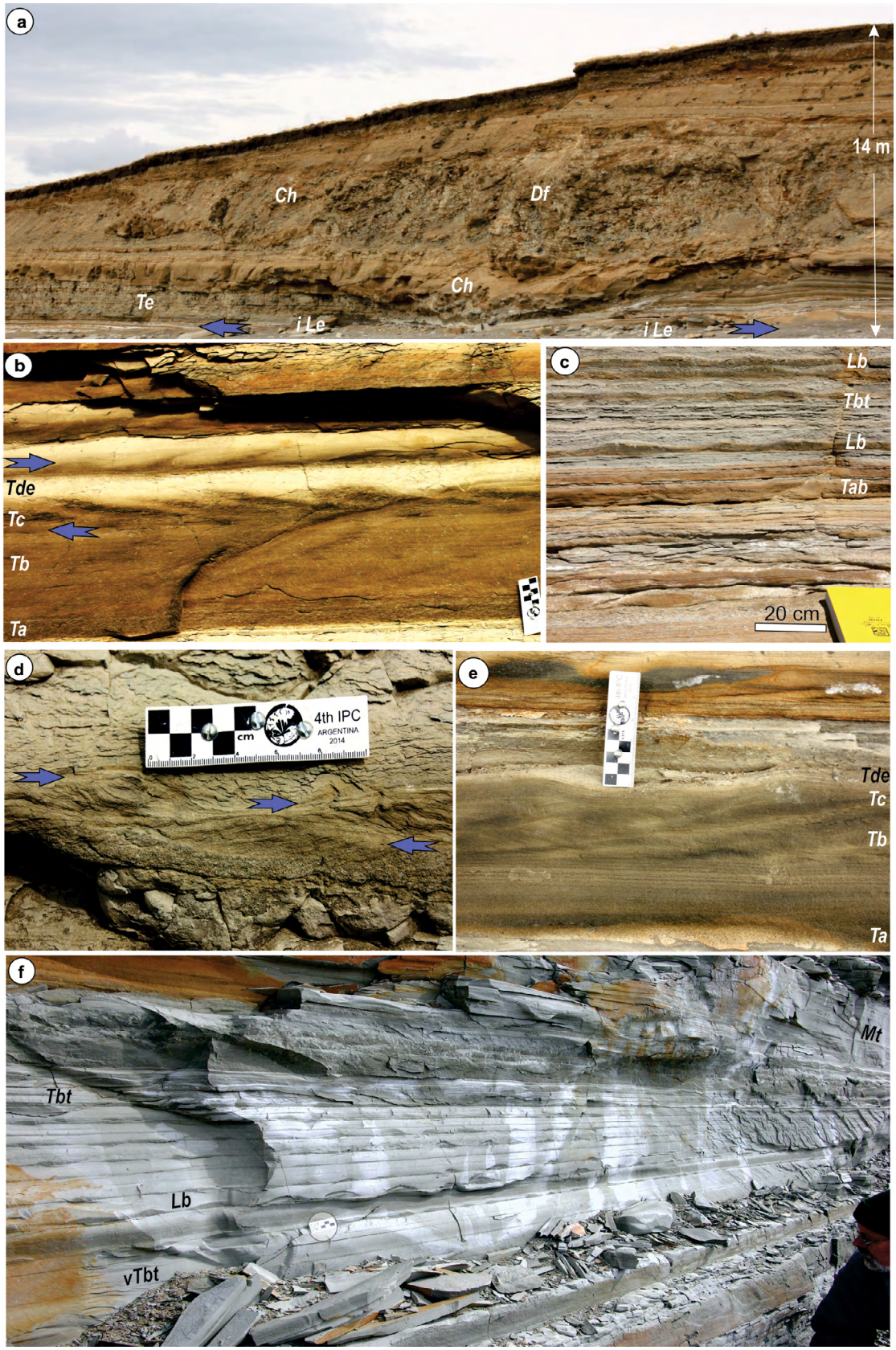

Figure 11: Internal levee and terrace architectural sub-elements. a) General view showing relationships among channel fill (Ch), partly with basal cohesive debrites (Df); terraces (Te) and internal levees (iLe) architectural sub-elements; b-f) Sedimentary facies of internal levees (b, d-f) and terraces (c). Internal levee proximal turbidites commonly record complete Bouma divisions (Ta-d/e). Notice paleoflow reversal (blue arrows) in adjacent beds (b) or in the same bed (d). In f, distal, thin-bedded (Tbt) or very thin-bedded (vTbt) turbidites record thick muddy divisions and starved ripples (Lb, lenticular bedding), circled scale in cm. Terrace deposits (c) record similar thin-bedded turbidites.

11e), the distribution of which show a gradual base-cut-out pattern, being progressively replaced by T*bcd*, T*cd*, and finally, several tens of meters away from the channel thalweg, by muddy turbidites (Fig. 10). Near the channel thalweg, climbing ripples are common in the T*c* Bouma division and typically display opposite paleocurrent flows, sometimes the reversal

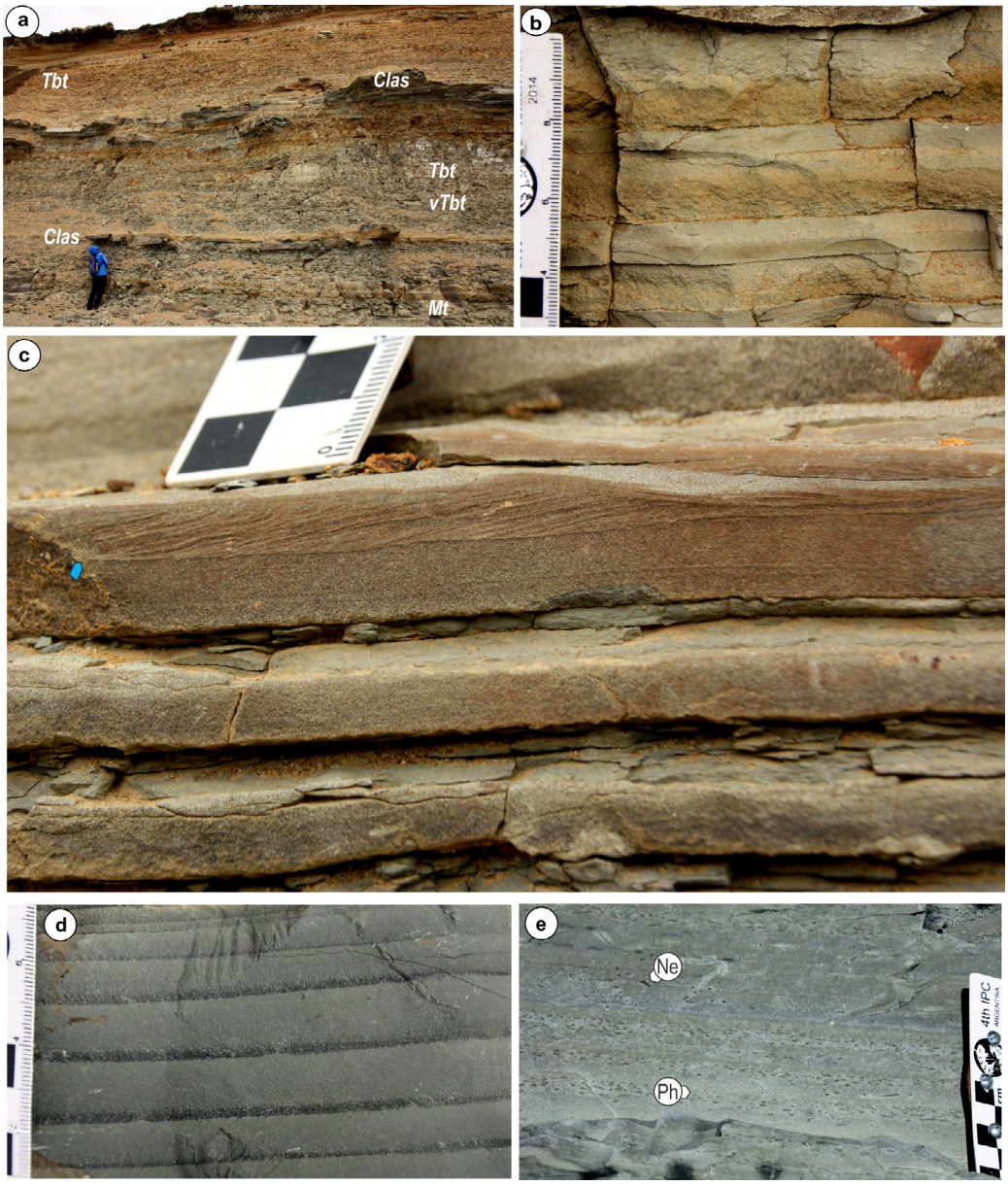

Figure 12: External levee architectural element. a) Outcrop SE of Cabo Auricosta (See Figure 7c). Sedimentary facies display three variations of thin-bedded turbidites: variation 1, muddy turbidites (Mt); variation 2, silty muddy turbidites (vTbt); variation 3 delicate thin-bedded turbidites (Tbt). Sandy, top-cut-out, classical turbidites (Clas) are scarce; b-c) Detail of variation 3, thin-bedded turbidites. Notice grain-size break (arrow) between Tb-Tc divisions; d-e) Variations 2 (d) and 1 (e) of thin-bedded turbidites. Notice prominent bioturbation, Nereites (Ne) and *Phycosiphon* (Ph), in variation 1 (e). Scale in cm.

is present even in the same bed (Figs 10-11). Away from the channel, the distal mud-rich turbidites commonly bear lenticular structures, with isolated, small ripples (starved ripples) dispersed in mud (Fig. 11f). Paleocurrent vectors measured from climbing ripples (Fig. 2) indicate paleoflows directed mainly to the SE, with slight deviations from those of the channel fill architectural sub-element. Some internal levee paleocurrents are directed to the NW, representing reflection and interaction of paleoflows with the channel belt topography (cf. Kane and Hodgson 2011).

Terraces consist of tabular thin-bedded turbidites that generally rest on a subtle, nearly flat erosive surface (Figs. 6b, 8c) or, rarely, on notable erosion surfaces with superimposed relatively large dunes (Fig. 9b). The sedimentary facies could only be observed in one case (Fig. 11c) and they have an arrangement quite similar to those of the distal internal levees. The observed architectures and sedimentary facies of internal levees and terraces are consistent and totally support the conclusions established by Kane and Hodgson (2011) and Hansen et al. (2015) for similar depositional sub-elements, mainly exposed in the Cretaceous of Baja California and the Permian of the Karoo Basin.

Basal slumps sub-element - heterolithic beds and pebbly mudstone: At a few places the base of the channel complex rests on a distinctive deposit (e.g., deposit 1, Fig. 6a), consisting mainly of large slumps of muddy blocks and cohesive debrites. This deposit is best exposed to the NW of Cabo Viamonte, but it was also observed to the SE, between

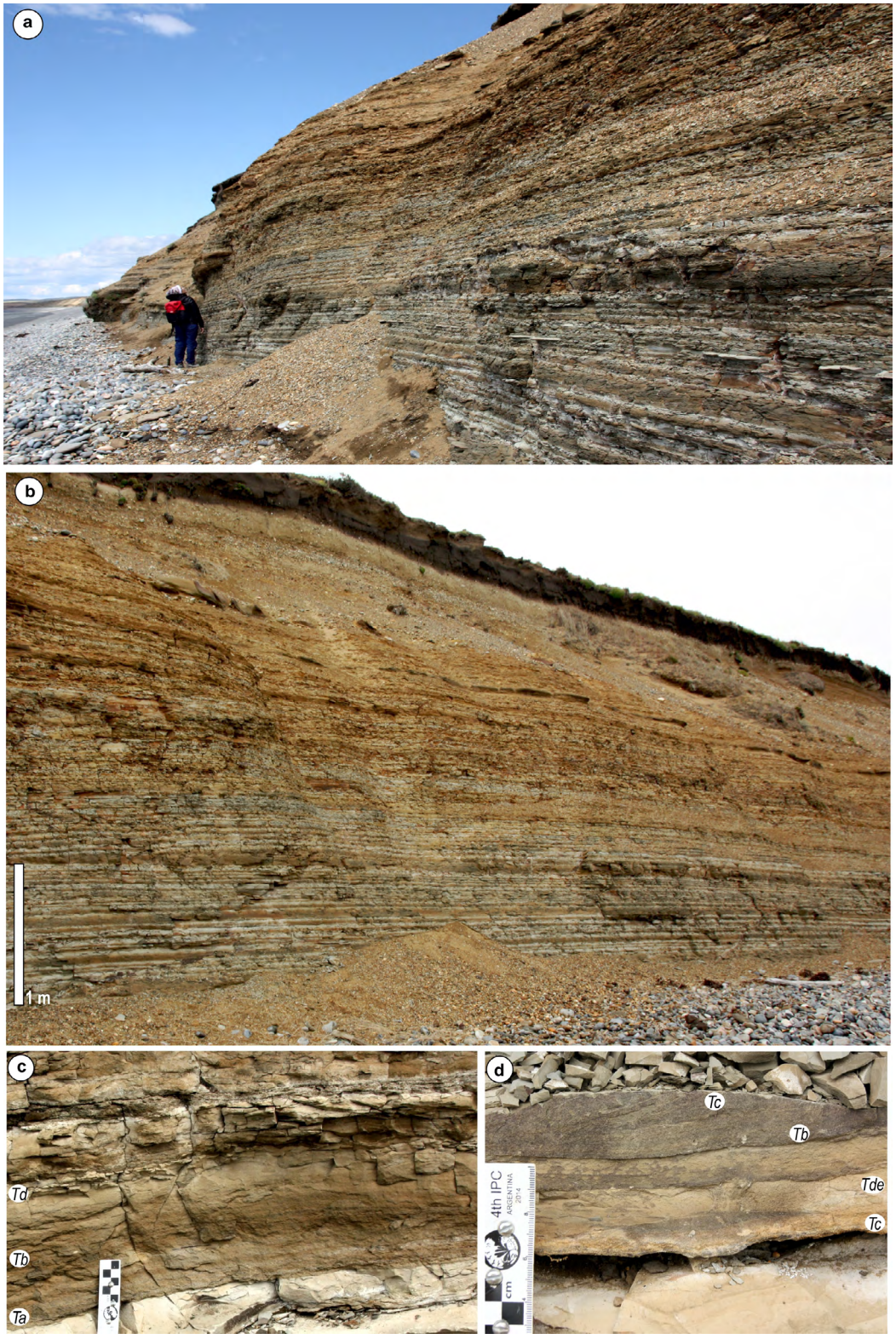

Figure 13: External levee architectural element. a-b) Rhythmical stratification and typical fining- and thinning-upward trend of the thin-bedded turbidite facies NW of Cabo Ewan (See figure 3); c-d) Detailed view of the lower and thick Ta-d turbidites (c) and the upper thin-bedded, Tb-c, Tc-de turbidites (d). Scale in cm.

Cabo Viamonte and Cabo Ewan. In all these sites, the basal slump-debrite lies just underneath the erosive surface of the channel complex and is covered by both coarse-grained conglomerate and breccia of the channel fill architectural sub-element and fine-grained muddy deposits of the internal levee. The basal slump-debrite has a exposed thickness of about 3 m; its base is not exposed. The most notable lithology (Fig. 7a) consists of large-scale, decimeter- to meter-sized slump blocks of deformed laminated thin-bedded turbidites displaying synsedimentary folds. The fine-grained sandstone

division of the thin-bedded turbidites commonly has climbing ripples and some mudstone horizons bear a dense bioturbation, mainly *Phycosiphon and Nereites*. In some areas, there are angular, thinly-laminated muddy intraclasts, 0.1-0.30 m in size, forming the matrix between large blocks. Scarce exposures record massive cohesive debrites, consisting of rounded pebbles to granules of allochthonous slate, quartz vein, and rhyolite floating in an abundant muddy matrix (Fig. 7a).

Due to its reduced thickness and patchy distribution this basal slump sub-element is difficult to interpret. The stratigraphic position beneath the dominant architectural sub-elements of the channel complex, the component facies dominated by thin-bedded turbidites, and the inferred large areal extension suggest either: (1) a previous, preavulsion deposit (levees?) of an older channel complex or (2) slump areas of levees within the same, overlying channel complex.

External levee

Within this architectural element, large wedge-shaped sedimentary bodies, comprising graded fine-grained, thin-bedded turbidites form continuous exposures, more than 1 km long and 20-30 m thick (Figs. 2, 6c). Component sedimentary facies are highly distinctive and dominated by thin-bedded turbidites, which commonly include the following variations: (1) centimeter- to decimeter-thick laminated muddy turbidites; (2) centimeter-thick silty muddy turbidites; (3) centimeter-thick *Tb-d/e* turbidites; and (4) subordinated, decimeter-thick, top-cut-out T*a-c* classical, sandy turbidites (Figs. 12, 13).

Variation (1) consists of a basal, very thin, 1-3 mm thick, siltstone lamina followed by a centimeter-thick, laminated mudstone division, which is generally bioturbated (Fig. 12e). Variation (2) is transitional with the former and consists of a basal centimeter-thick very fine-grained sandstone or siltstone followed by a much thicker graded mudstone (Fig. 12d). The basal, coarser lamina has a sharp contact, with the basal surface preserving delicate casting of simple grazing trace fossils, similar to *Helminthoidichnites*. Variation (3) comprises very delicate thin-bedded turbidites that consist of a sharp base, above which is a centimeter-thick laminated, fine-grained sandstone interrupted at its top by a delicate, sharply defined surface that marks a grain-size break with the following centimeter-thick, ripple cross-laminated very fine sandstone. The bed ends with laminated or massive mudstone (Figs. 12b-c, 13d). The basal division also records casts of trace fossils similar to that of variation (2) and possible wrinkle structures. Variations of thin-bedded turbidites (1) to (3) are transitional and form meter-thick repetitive packages with no evident trend, except for their preferred occurrences in the mid-upper part of the levee-column, seemingly in a distal position respect to the channel belt. Variation (4) turbidites are scarce in this architectural element, some of them form conspicuous horizons (Fig. 12a) of two or three, amalgamated and bioturbated beds, which consist of decimeter-thick classical sandy turbidites lacking the muddy upper divisions. Others, generally located at the base of the levee succession near the channel margins, consist of classical T*a-d/e* turbidites (Fig. 13c). Both bear flute casts and ripple cross-lamination and different trace fossil assemblages, dominated by *Scolicia*, *Phymatoderma, Chondrites* and graphoglyptids (López Cabrera and Olivero in preparation).

Paleocurrent vectors measured from flute casts and climbing ripples, consistently indicate paleoflows directed to the SE, with minor deviation to the ESE and SSE (Fig. 2). As inferred from its highly distinctive sedimentary facies, paleocurrents, and spatial relationships with channel belt architectural sub-elements, this architectural element is interpreted as external levee deposits. All these features are consistent with those interpreted from external levees in outcrop and subsurface studies (e.g. Kane and Hodgson 2011, Hansen et al. 2015, and the bibliography therein). Two cases, which do not include all these features but are also interpreted as belonging to this architectural element, correspond to the particular outcrops mentioned in the description of the gully axis architectural element in the Cabo Santa Inés and Cabo Viamonte localities. These particular outcrops (Localities 93 and 121 in Figs. 2, 3), have sedimentary facies typical of the external levee architectural element and also record a similar paleocurrent pattern, hence, they are tentatively included within this architectural element.

The external levee deposits located along the cliff depicted in Figure 6c could be misleading in the sense that they show strata gently dipping to the NNW and paleocurrents generally directed to the SE, as if paleoflows were climbing updip the levee flank. However, this is not the case as this is an apparent dip direction, with true dip-direction oriented to the WSW. Due to the great inertia inherent to large gravity flows, the flow that spills over the external levee deviate slightly from the orientation of the channel axis (cf. Posamentier and Walker 2006, Kane et al. 2007). Therefore, in the cliff section of Figure 6c paleoflows spilling over the levee crest were still directed to the SSE, moving obliquely down the levee flank. This slight flow deviation is indicated by the paleoflow vectors of the external levee at localities 75 and 837, and those of the adjacent channel at localities 83 and 72 (Fig. 2).

INTERPLAY BETWEEN TRANSVERSE AND LONGITUDINAL DEPOSITIONAL SYSTEMS

During cessation of contractional deformation and encompassing most of the Miocene, the basin physiography at the latitude of the studied area consisted of an elevated NW-SE-oriented area exposed to subaerial erosion (the Fuegian Andes), a deep-marine foreland basin located outboard of the thrust-fold belt front, and a submerged topographic high of general N-S orientation (the Rio Chico Arch), separating the Austral and Malvinas basins (Fig. 1a; Biddle et al. 1986, Galeazzi 1998, Torres Carbonell and Olivero 2019, Lovecchio et al. 2019). The basin sea-bottom profile approximated a ramp, or clinoform, several hundreds of meters high, connecting shallower areas to the SW and deeper areas in the foredeep to the NE, characterizing the typical Oligocene-Miocene basin fill architecture displayed in seismic lines (e.g. Fig. 1b, Biddle et al. 1986, Robbiano et al. 1996, Barros et al. 2018). A platform on the proximal, shallower edge of the ramp was absent or much reduced and NE-directed progradation of these oblique, ramp clinoforms originated the dominantly muddy slope clinothems of the Cabo Domingo Group, previously included in the latest Oligocene-Miocene S1-S4 (Ponce et al. 2008) and sub-package 1 of Torres Carbonell and Olivero (2019). Due to the general absence of inland outcrops, this progradational, transverse slope system is mostly known from oil-exploration wells (Biddle et al. 1986, Barros et al. 2018 and references therein) and from a narrow belt of exposures along the Atlantic coast (Malumián and Olivero 2006, Ponce et al. 2008, Ponce and Carmona 2011a). North of the study area, the progradational submarine ramp system is covered by Miocene progradational-aggradational deltaic clinothems in an overfilled basin, which was denominated sub-package 2 by Torres Carbonell and Olivero (2019). These deltaic clinoforms are evident in seismic lines (e.g. Galeazzi 1998, Robbiano et al. 1996) and are of much lower height, about 50-60 m, than the several hundreds of meters high clinoforms of the progradational sub-package 1.

In both, progradational and progradational-agradational transverse systems Torres Carbonell and Olivero (2019) envisaged a long-lived SE directed, channelized axial system topographically confined between the NE facing submarine ramp and the Rio Chico Arch. This topographic high apparently functioned as a rampart during the Miocene at the study area, rerouting to the SE the sediments moving through the transverse slope system. The results of our study in the type area of the Viamonte Formation improve upon this previous

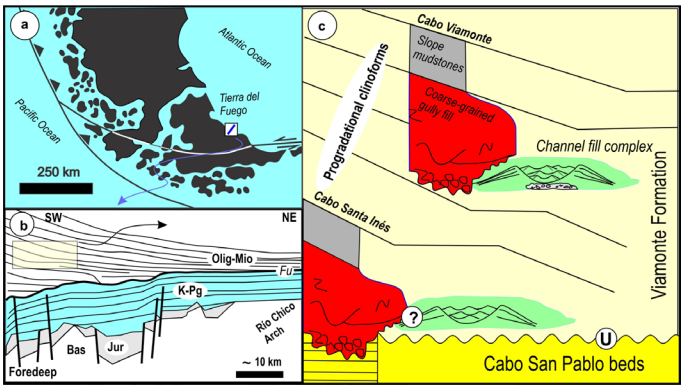

Figure 14: Schematic depositional model of the Viamonte Formation. a) Approximate location of figure 14b (rectangle); b) Large-scale depositional architecture of the studied depositional systems at the slope breaks of foredeep clinoforms; Bas: Paleozoic basement; Jur: Jurassic; K-Pg: Cretaceous-Paleogene; Olig-Mio: Oligocene-Miocene; Fu: Foreland unconformity. Inspired in seismic sections shown in Galeazzi (1998) and Torres Carbonell et al. (2017b); c) Stratigraphy and interplay among the different architectural elements interpreted for the Viamonte Formation. Note that the Formation includes at least two intervals of coarse-grained, gully fill deposits, fine-grained slope deposits, and channel fill complexes. U: unconformity.

work, supporting a clear distinction in terms of sedimentary facies, paleocurrents, and stratigraphic relationships between transverse gullies-slope deposits and axial channel belt-external levee deposits (Figs. 1, 2, 14).

The sedimentary facies of the gully and other slope deposits architectural element are highly distinctive and dominated by thick, disorganized MTDs packages (Figs. 3-5), including debris avalanche deposits with exotic, albeit of basinal provenance, blocks; cohesive mud-rich debrites with autochthonous and allochthonous pebbles and cobbles; and blocky flow and slump deposits, with large deformed blocks of local lithologies. Being typical of the gully axis architectural sub-element, these facies are in general common in slope settings of foreland basins and are the dominant lithologies filling the bulk of submarine canyons and gullies (Posamentier and Walker 2006, Nelson et al. 2011). They are well-known in several submarine slope depositional settings of orogenic margins around the world, for example the Apennines (Piazza and Tinterri 2020), the Alps (Kremer et al. 2018), the Gull Island Formation, Shannon Basin in Ireland (Martinsen et al. 2003, Posamentier and Martinsen 2011), among others. Cyclic steps, formed by cross-bedded backsets climbing up the bottom of gully axis architectural sub-element (e.g. Fig. 5a-c), are similar to cross-bedded backsets deposits of slope channels in the Hecho Group, Spain (Postma et al. 2014). The muddier and finer-grained mudstones and thin turbidites capping the gullies, the abandonment facies, may form the bulk of the transverse clinoforms lithologies drilled by exploration wells in the interior of the island of Tierra del Fuego.

Compared with the gullies and other slope deposits architectural element, the channel belt and limiting external levees of the Viamonte Formation display very different sedimentary facies dominated by lenticular strata bearing well organized high-density sandy turbidites; lateral accretion packages; thin bedded turbidites forming terrace and internal levees; and extended external levee deposits of thick and bioturbated thin bedded turbidites (Figs. 6-13). Well-studied leveed channels depositional settings, such as the Permian Karroo Basin and the Cretaceous Rosario Formation, Mexico (e.g. Kane and Hodgson 2011, Hansen et al. 2015) record sedimentary facies and architectures remarkably similar to those of the Viamonte Formation. In addition to sedimentary facies, nearly orthogonal paleoflow directions clearly distinguish gullies and other slope deposits from channel belt/external levee architectural elements (Fig. 2).

Despite their striking differences in sedimentary facies, architectures, and flow orientation these architectural elements are generally not imaged in 2D seismic lines, probably because the scale of most them is beyond seismic resolution. Nonetheless, a few published 3D seismic data do clearly show Oligocene NW-SE oriented channel belts in the studied area (Fig. 1d; Torres Carbonell and Olivero 2019). Moreover, Barros et al. (2018) published seismic sections from the same area imaging a NW-SE belt of incised channels. Both of these subsurface channel belts imaged from 3D seismic data are older than the surficial channel belt mapped in the Atlantic coast (Fig. 2), suggesting that long-lived axial channel belt depositional systems and transverse prograding slope clinothems were simultaneously developing, as it is schematically shown in Figure 14c for the Viamonte Formation.

The gullies shown in the scheme of Figure 14c were not yet detected in published seismic reflection images. However, the relatively large, canyon-shaped incisions constrained by steep-walls and filled with impressive MTD-dominated sedimentary facies (Figs. 2, 3a-b) attest the presence of transverse gullies in the Viamonte Formation. The gully steep walls were carved either in the Cabo San Pablo beds (Fig. 3a) or in the channel-levee complex (Fig. 3b). In both cases, the basal deposits lying just above the basal gully erosional surface consist of thin-bedded, carbonaceous, turbidites typical of the external levee architectural element (Fig. 3). Furthermore, paleocurrent vectors in climbing ripples of these thin-bedded turbidites filling the gully, consistently indicate axial, SE-directed paleoflows (localities 93, 121 in Fig. 2), which is in marked contrast with the general NE-directed paleoflows in the transverse gully-fill sedimentary facies. These features suggest that once the gully was originated, the still sediment-free depression was filled with thin-bedded turbidites deposited by axial gravity flows. Travelling along the axial channel belt, the more diluted part of these gravity flows spilling over the levee crest entered into the adjacent transverse depression filling the gully. A similar case is known in the Puchkirchen Formation of the Alpine Molasse Basin in Austria (Hubbard et al. 2009, Masalimova et al. 2015, Kremer et al. 2018). The simultaneous interplay of transverse and axial depositional systems is also supported by the outstanding transverse debris-flow/blocky-flow deposits (Fig. 3b-d), with deformed boulders of thin-bedded turbidites detached from the sole, and covered by similar, axial thin-bedded carbonaceous turbidites, lapping markedly onto its upper surface.

Even though transversely emplaced MTDs form the bulk of the gully axis and reach a combined thickness in excess of 65 m (Fig. 3a-b), this thickness represents amalgamated event deposits. The thickest individual deposit reaches a minimum thickness of only a few meters (e.g. Fig. 4d), suggesting that individual MTDs were not volumetrically important as to block the axial leveed channels. Huge MTDs that spread over hundreds of kilometers and reach tens of meters in thickness, capable of blocking channels and forming ponded basins, are controlled by a number of variables, among which the axial gradient of the feeder canyon is of prime importance (Nelson et al. 2011). In a survey of the interplay between mass-transport and turbidite-system deposits in recent different margin settings, Nelson et al. (2011) concluded that largest MTDs are associated with irregular, steep gradients (5-9°) in passive margins; whereas active tectonic margins with more regular and less steep gradients (1-5°) are less prone do develop large MTDs. The gradient of deep-marine clinoforms in the Oligocene-Miocene transverse systems of Tierra del Fuego is generally between of 1-2° (Torres Carbonell and Olivero 2019), and thus relatively low-sized MTDs should be expected. Hence, the fact that MTDs forming the gully axis fill in the Viamonte Formation are relatively small, supports the interpretation of Nelson et al. (2011).

Another consequence of the relatively low gradient of transverse clinoforms is that axial leveed channels were probably not necessarily restricted to the toe of the clinoforms. With such a low gradient of about 1-2°, processes such as differential compaction, or displacement of deep faults accommodating large overburdens, are prone to cause topographic irregularities leading to steps or clinoform breaks along the transverse ramp (Fig. 14b-c). Nearby our study area, such processes are interpreted from seismic-imaged early Paleogene extensional growth strata above normal faults that accommodate flexure of the foreland basin basement (Torres Carbonell

et al. 2017b). These normal faults are reactivated structures inherited from the Late Jurassic rifting phase, and mostly oriented NW-SE (Biddle et al. 1986, Galeazzi 1998, Torres Carbonell et al. 2017b, Lovecchio et al. 2019). It is therefore suggested that similar fault reactivation caused by the weight of a thick sedimentary wedge during the Neogene may constitute one of the controls of clinoform breaks formation, constraining the location of SE-directed axial channel belts at the study area. Since several of these slope breaks are imaged across the transverse clinoforms of the Austral and Malvinas basins (e.g. Fig. 14, Galeazzi 1998, Baristeas et al. 2013, Barros et al. 2018), probably the location of axial channel belts were not just restricted to the base of the clinoforms, suggesting that leveed channels could be more widespread than previously thought in the foreland basins of Tierra del Fuego (e.g. Torres Carbonell and Olivero 2019).

CONCLUSIONS

The main conclusions of our study could be summarized as follows.

At the type section, designated in the coastal area between Cabo Auricosta and Cabo Santa Inés, the base of the Miocene Viamonte Formation is a deeply incised unconformity with a relief of more than 40 m carved into the Cabo San Pablo beds. The Formation records a notable architectural variability, characterized by lenticular (channelized) geometries present at various scales. The largest channelized incisions are slope gullies oriented perpendicular to the thrust-fold belt front of the Austral basin, such as those recognized at Cabo Santa Inés and Cabo Viamonte. These erosional conduits have steep walls and minimum cross-sections about 2-3 km wide and 70-100 m deep. At a lower scale, other incisions correspond to a channel belt running parallel to the axis of the Austral basin foredeep. Each channel-form presents widths of about 500 m and thicknesses of 30-40 m. Flanking the channel belt is a wedge-shaped sedimentary body that corresponds to the external levee. Based on scale, external geometry, dominant lithology and paleocurrents, three highly distinctive, higher-rank architectural elements are recognized in the Viamonte Formation: (A) gullies and other slope deposits; (B) channel belt; and (C) external levee.

The element gullies and other slope deposits (A), is subdivided into gully axis, gully off-axis/gully margin, and slope-gully abandonment sub-elements.

Gully axis deposits consist of more than 60 m of amalgamated lenticular MTDs, commonly including debris avalanche, cohesive debris flow, blocky flow, and large slump deposits. Less common are large-scale climbing dunes and upslope dipping strata (backset stratification) interpreted as cyclic steps.

Gully off-axis/gully margin deposits consist of almost tabular pebble conglomerate, pebbly sandstone, and sandstone beds that away from the gully axis split into thinner alternations of sandstone and mudstone beds. Slope-gully abandonment deposits consist of well-stratified sandstones and mudstones with localized channelized conglomerates and slumps.

Paleocurrents measured from climbing dunes, clast imbrication, and flute casts are consistently directed to the NNW-NE.

The channel belt architectural element (B) is subdivided into channel fill, lateral accretion deposits (LADs), internal-levee/terrace, and basal slumps sub-elements.

Channel fills display characteristic fining- and thinning-upward trends, comprising basal coarse-grained facies that grade upwards to interbedded, sandy turbidite and mudstone.

LADs consist of inclined deposits that dip laterally away from the channel margin and comprise a lower coarse-grained facies that grade upward along the inclined stratification to rhythmic interbedding of progressively thinning sandstone-mudstone turbidites.

Internal-levee/terrace deposits are dominantly thin-bedded turbidites, portraying wedge-shaped geometries in internal levees and tabular horizontal deposits in terraces. Paleocurrents in the channel belt are oriented to the SE. Due to reflections and deflections against topographic irregularities within the channel belt, internal levees also record opposite, NW-oriented paleoflows.

The external levee architectural element (C) comprises dominantly thick, wedge-shaped packages of thin-bedded turbidite flanking the channel belt. Paleocurrents measured from climbing ripples and flute casts are oriented to the SE, with minor deviations with respect to paleoflows recorded in the channel belt.

Mapping and spatial integration of the higher-rank architectural elements and lower-rank constituent sub-elements, made possible their linkage into transverse and axial, major depositional systems. The architectural element (A) gullies and other slope deposits, characterizes the transverse depositional system; while the architectural elements(B) channel belt and (C) external levee, characterizes the axial depositional systems. In the transverse depositional system, large NE-prograding, oblique low-angle (c. 1-2°) dipping clinoforms terminate in onlap against the foreland unconformity. The interplay between transverse and axial systems is evidenced by

the activity of gravity flows, which while travelling along the axial channel belt, spilled over the levee crest, entering into the adjacent transverse gully, and depositing there thin-bedded turbidites above the basal gully erosive surface. This interplay is also evidenced in the youngest Cabo Viamonte gully fill depositional element, the basal erosion of which is carved into the axial, external levee depositional element of the Viamonte Formation. The low-gradient of the clinoforms that controlled MTDs deposition in the transverse system probably resulted in the relatively small size of the involved submarine landslides, with the consequent lack of generation of important topographic barriers capable of blocking the axial flows in the channel belt. Another consequence of the relatively low gradient of transverse clinoforms is that axial leveed channels were probably not necessarily restricted to the toe of the clinoforms. Differential compaction, or displacement of deep faults accommodating large overburdens, are prone to cause topographic irregularities leading to steps or clinoform breaks along the transverse ramp, promoting the development of axial channel belts. Accordingly leveed channels could be more widespread than previously thought in the foreland Austral basin of Tierra del Fuego.

ACKNOWLEDGMENTS

We thank the facilities provided by T. Ayerza and A. Goodal, Estancia Viamonte and S. Bilbao and J. Contreras, Estancia Inés. M. Rodríguez (UNTDF) helped during field works at Cabo Santa Inés. We deeply thank the continuous support during field work of M.I. López-Cabrera (CADIC-CONICET), particularly for her input on trace fossils and environmental controls. Reviews by S. Marenssi, an anonymous reviewer, and Chief Editor D. Kietzmann have greatly improve the reading clarity of the original MS. We acknowledge the financial support by PIDUNTDF-A1 and PUE 2016-CONICET (CADIC).

REFERENCES

Allen, P.A. and Homewood, P. 1986. Foreland Basins. The International Association of Sedimentologists, Special Publication, 8, 453 p., Oxford.

Arnott, R.W.C. 2007. Stratal architecture and origin of lateral accretion deposits (LADs) and conterminuous inner-bank levee deposits in a base-of-slope sinuous channel, lower Isaac Formation (Neoproterozoic), East-Central British Columbia, Canada. Marine and Petroleum Geology 24: 515-528.

Bargo, M.S., Cerdeño, E., Olivero, E.B., López Cabrera, M.I., Reguero, M.A. and Vizcaíno, S.F. 2018. Primer registro de Astrapotheriidae (Mammalia, Astrapotheria) de la Formación Cullen (Mioceno temprano) de Tierra del Fuego. Reunión de Comunicaciones de la Asociación Paleontológica Argentina, Libro de Resúmenes, Puerto Madryn.

Barbeau, D.L., Olivero, E.B., Swanson-Hysell, N.L., Zahid, K.M., Murray, K.E. and Gehrels, G.E. 2009. Detrital-zircon geochronology of the eastern Magallanes foreland basin: implications for Eocene kinematics of the northern Scotia Arc and Drake Passage. Earth Planetary Science Letters 284: 489-503.

Baristeas, N., Anka, Z., di Primio, R., Rodriguez, J.F., Marchal, D. and Dominguez, F. 2013. New insights into the tectono-stratigraphic evolution of the Malvinas Basin, offshore of the southernmost Argentinean continental margin. Tectonophysics 604: 280-295.

Barros, P., Marino, J., Miller, M., Angelozzi, G., Ronchi, D., Hiriart, L. and Giampaoli, P. 2018. Integración de nuevos datos bioestratigráficos en un modelo regional sismoestratigráfico de la Cuenca Austral Fueguina. 10° Congreso de Exploración y Desarrollo de Hidrocarburos, Sesiones Generales: "Energía y Sociedad, aliados inseparables" Instituto Argentino del Petróleo y el Gas (IAPG): 835-856, Mendoza.

Bedoya-Agudelo, E.L. 2019. Asociaciones de nanofósiles calcáreos del Paleoceno-Mioceno de Tierra del Fuego. Bioestratigrafía, Paleoecología y Paleooceanografía. Tesis Doctoral, Universidad de Buenos Aires (unpublished), 491p., Buenos Aires.

Biddle, K.T., Uliana, M.A., Mitchum Jr., R.M., Fitzgerald, M.G. and Wright, R.C. 1986. The stratigraphy and structural evolution of the central and eastern Magallanes basin, southern South America. In: Allen, P.A. and Homewood, P. (eds.), Foreland Basins. International Association of Sedimentologists. Special Publication 8: 41-66, Oxford.

Crane, W.H. and Lowe, D.R. 2008. Architecture and evolution of the Paine channel complex, Cerro Toro formation (Upper Cretaceous), Silla syncline, Magallanes basin, Chile. Sedimentology 55: 979-1009.

Dalziel, I.W.D. 1981. Back-arc extension in the southern Andes: a review and critical reappraisal. Philosophical Transactions of the Royal Society, London, Ser. A Mathematical and Physical Sciences 300: 319-335.

Decelles, P.G. and Giles, K.A. 1996. Foreland basin systems. Basin Research 8: 105-123.

Festa, A., Ogata, K., Pini, G.A., Dilek, Y. and Alonso, J.L. 2016. Origin and significance of olistostromes in the evolution of orogenic belts: A global synthesis. Gondwana Research 39: 180-203.

Fosdick, J.C., Graham, S.A. and Hilley, G.E. 2014. Influence of attenuated lithosphere and sediment loading on flexure of the deep-water Magallanes retroarc foreland basin, Southern Andes. Tectonics 33: 2505-2525.

Galeazzi, J.S. 1998. Structural and stratigraphic evolution of the western Malvinas Basin, Argentina. American Association of Petroleum Geologists, Bulletin 82: 596-636.

Ghiglione, M.C., Likerman, J., Barberon, V., Giambiagi, L.B., Aguirre-Urreta, B. and Suárez, F. 2014. Geodynamic context for the deposition of coarse-grained deep-water axial channel systems in the Patagonian Andes. Basin Research 26: 726-745.

Hansen, L.A.S., Callow, R.H.T., Kane, I., Gamberi, F., Rovere, M., Cronin, B.T. and Kneller, B. 2015. Genesis and character of thin-bedded turbidites associated with submarine channels. Marine and Petroleum Geology 67: 852-879.

Hervé, F., Pankhurst, R.J., Fanning, C.M., Calderón, M., and Yaxley, G.M. 2007. The South Patagonian batholith: 150 my of granite magmatism on a plate margin. Lithos 97: 373-394.

Hubbard, S.M., Romans, B.W. and Graham, S.A. 2008. Deep-water foreland basin deposits of the Cerro Toro Formation, Magallanes Basin, Chile: architectural elements of a sinuous basin axial channel belt. Sedimentology 55: 1333-1359.

Hubbard, S.M., De Ruig, M.J. and Graham, S.A. 2009. Confined channel–levee complex development in an elongate depo-center: Deep-water Tertiary strata of the Austrian Molasse basin. Marine and Petroleum Geology 26: 85-112.

Kane, I.A., Kneller, B.C., Dykstra, M., Kassem, A. and McCaffrey, W.D. 2007. Anatomy of a submarine slope channel-levee: an example from Upper Cretaceous slope sediments, Rosario Formation, Baja California, Mexico. Marine and Petroleum Geology 24: 540-563.

Kane, I. and Hodgson, D. 2011. Sedimentological criteria to differentiate submarine channel levee subenvironments: Exhumed examples from the Rosario Fm. (Upper Cretaceous) of Baja California, Mexico, and the Fort Brown Fm. (Permian), Karoo Basin, S. Africa. Marine and Petroleum Geology 28: 807-823.

Klepeis, K.A., Betka, P., Clarke, G.,Fanning, M., Hervé, F., Rojas, L., Mpodozis, C. and Thomson, S. 2010. Continental underthrusting and obduction during the Cretaceous closure of the Rocas Verdes rift basin, Cordillera Darwin, Patagonian Andes. Tectonics 29, TC3014.

Kremer, C.H., McHargue, T., Scheucher, L. and Graham, S.A. 2018. Transversely-sourced mass-transport deposits and stratigraphic evolution of a foreland submarine channel system: Deep-water tertiary strata of the Austrian Molasse Basin. Marine and Petroleum Geology 92: 1-19.

López Cabrera, M.I., Olivero, E.B., Carmona, N.B. and Ponce, J.J. 2008. Cenozoic trace fossils of the Cruziana, Zoophycos, and Nereites ichnofacies from the Fuegian Andes, Argentina. Ameghiniana 45: 377-392.

López Cabrera, M.I. and Olivero, E.B. 2018. Morphological variability in the gastropod Perissodonta martens (=Struthiolarella) from the Early Miocene of Tierra del Fuego. Reunión de Comunicaciones de la Asociación Paleontológica Argentina, Libro de Resúmenes, Puerto Madryn.

Lovecchio, J.P., Naipauer, M., Cayo, L.E., Rohais, S., Giunta D., Flores, G., Gerster, R., Bolatti, N.D., Joseph, P., Valencia, V.A. and Ramos, V.A. 2019. Rifting evolution of the Malvinas basin, offshore Argentina: New constrains from zircon U–Pb geochronology and seismic characterization. Journal of South American Earth Sciences 95: 102253.

Malkowski, M.A., Schwartz, T.M., Sharman, G.R., Sickmann, Z.T. and Graham, S.A. 2017. Stratigraphic and provenance variations in the early evolution of the Magallanes-Austral foreland basin: Implications for the role of longitudinal versus transverse sediment dispersal during arc-continent collision. Geological Society of America Bulletin 129: 349-371.

McAtamney, J., Klepeis, K., Mehrtens, C., Thomson, S., Betka, P., Rojas, L. and Snyder, S. 2011. Along-strike variability of back-arc basin collapse and the initiation of sedimentation in the Magallanes foreland basin, southernmost Andes (53–54.5°S). Tectonics 30: TC5001.

Malumián, N. 2002. El terciario marino de la provincia de Santa Cruz. In: Haller, M.J. (ed.). Geología y Recursos Naturales de Santa Cruz, 15° Congreso Geológico Argentino, Relatorio: 237-244, Buenos Aires.

Malumián, N. and Olivero, E.B. 2006. El Grupo Cabo Domingo, Tierra del Fuego: bioestratigrafia, paleoambientes y acontecimientos del Eoceno-Mioceno marino. Revista de la Asociación Geológica Argentina 61: 139-160.

Martinioni, D.R. 2010. Estratigrafía y sedimentología del Mesozoico Superior-Paleógeno de la Sierra de Beauvoir y adyacencias, Isla Grande de Tierra del Fuego, Argentina. Tesis Doctoral, Universidad de Buenos Aires (unpublished), 195p., Buenos Aires.

Martinsen, O.J., Lien, T., Walker, R.C. and Collinson, J.D. 2003. Facies and sequential organization of a mudstone-dominated slope and basin floor succession: The Gull Island Formation, Shannon basin, Ireland. Marine and Petroleum Geology 20: 789-807.

Masalimova, L.U., Lowe, D.R., Mchargue, T. and Derksen, R. 2015. Interplay between an axial channel belt, slope gullies and overbank deposition in the Puchkirchen Formation in the Molasse Basin, Austria. Sedimentology 62: 1717-1748.

Mulder, T. 2011. Gravity Processes and Deposits on Continental Slope, Rise and Abyssal Plains. In: Hüneke, H. and Mulder, T. (eds), Deep Sea Sediments. Elsevier, Developments in Sedimentology 63: 25-148.

Mutti, E. and Normark, W.R. 1991. An integrated approach to the study of turbidite systems. In:Weimer, P. and Link, H. (eds.), Seismic Facies and Sedimentary Processes of Submarine Fans and Turbidite Systems. Springer-Verlag: 75-106, New York.

Nelson, C.H., Escutia, C., Damuth, J.E. and Twichell, D.C. Jr. 2011. Interplay of mass-transport and turbidite-system deposits in different active tectonic and passive continental margin settings: external and local controlling factors. In: Shipp, R.C., Weimer, P. and Posamentier, H.W. (eds.), Mass-Transport Deposits in Deepwater Settings, SEPM Special Publication 96: 39-66 (CD-ROM).

Olivero, E.B. 2002. Petrografía sedimentaria de sistemas turbidíticos del Cretácico–Paleógeno, Andes Fueguinos: procedencia, volcanismo y deformación. 15° Congreso Geológico Argentino, Actas: 611-612. Calafate, Santa Cruz, Argentina.

Olivero, E.B. and López Cabrera, M.I. 2020. A new shallow-marine, high-latitude record of the trace fossil Macaronichnus in Miocene, reworked delta-front clinoforms, Punta Basílica, Tierra del Fuego, Argentina. Ichnos 27(4): 369-383.

Olivero, E.B. and Malumián, N. 1999. Eocene stratigraphy of southeastern Tierra del Fuego Island, Argentina. American Association of Petroleum Geologists, Bulletin 83: 295–313.

Olivero, E.B. and Malumián, N. 2008. Mesozoic-Cenozoic stratigraphy of the Fuegian Andes, Argentina. Geologica Acta 6: 5-18.

Olivero, E.B., Malumián, N., Palamarczuk, S. and Scasso, R.A. 2002. El Cretácico Superior-Paleógeno del área del Rio Bueno, costa atlántica de la Isla Grande de Tierra del Fuego. Revista de la Asociación Geológica Argentina 57: 199-218.

Olivero, E.B., Malumián, N. and Palamarczuk, S. 2003. Estratigrafia del Cretácico Superior-Paleoceno del área de Bahia Thetis, Andes fueguinos, Argentina: acontecimientos tectónicos y paleobiológicos. Revista Geológica de Chile 30: 245-263.

Olivero, E.B., López Cabrera, M.I. and Reguero, M.A. 2015. Icnología de los depósitos fluviales de la Formación Cullen (Mioceno, Tierra del Fuego) y su relación con la Formación Santa Cruz (Mioceno) de Patagonia. SLIC 2015, 3° Simposio Latinoamericano de Icnología. Colonia, Uruguay.

Piazza. A. and Tinterri, R. 2020. Mass-Transport Deposits in the Foredeep Basin of the Miocene Cervarola Sandstones Formation (Northern Apennines, Italy). In: Ogata, K., Festa, A. and Pini, G.A. (eds.), Submarine Landslides: Subaqueous Mass Transport Deposits from Outcrops to Seismic Profiles, American Geophysical Union, Geophysical Monograph 246: 27-44. John Wiley & Sons, Inc, New York.

Ponce, J.J. 2009. Análisis estratigráfico secuencial del Cenozoico de la Cordillera Fueguina, Tierra del Fuego, Argentina. Doctoral tesis, Universidad Nacional del Sur (unpublished), 245 p., Bahía Blanca.

Ponce J.J., Olivero E.B. and Martinioni D.R. 2008. Upper Oligocene–Miocene clinoforms of the foreland Austral Basin of Tierra del Fuego, Argentina: Stratigraphy, depositional sequences and architecture of the foredeep deposits. Journal of South American Earth Sciences 26: 36-54.

Ponce, J.J. and Carmona, N. B. 2011a. Miocene deep-marine hyperpycnal channel levee complexes, Tierra del Fuego, Argentina: Facies associations and architectural elements. In Slatt R.M. and Zavala, C. (eds.), Sediment transfer from shelf to deep water-Revisiting the delivery system: AAPG Studies in Geology 61: 75-93. Tulsa.

Ponce, J.J. and Carmona, N. B. 2011b. Coarse-grained sediment waves in hyperpycnal clinoform systems, Miocene of the Austral foreland basin, Argentina. Geology 39: 763-766.

Posamentier, H.W. and Walker, R.G. 2006. Deep-water turbidites and submarine fans. In: Posamentier, H.W. and Walker, R.G. (eds.), Facies Models Revisited. SEPM Special Publication 84 (CD-ROM).

Posamentier, H.W. and Martinsen, O.J. 2011. The character and genesis of submarine mass-transport deposits: insights from outcrop and 3D seismic data. In: Shipp, R.C., Weimer, P. and Posamentier, H.W. (eds), Mass-Transport Deposits in Deepwater Settings, SEPM Special Publication 96: 7-38 (CD-ROM).

Postma, G. and Cartigny, M. 2014. Supercritical and subcritical currents and their deposits – A synthesis. Geology 42: 987-990.

Postma, G., Kleverlaan, K. and Cartigny, M.J.B. 2014. Recognition of cyclic steps in sandy and gravelly turbidite sequences, and consequences for the Bouma facies model. Sedimentology 61: 2268-2290.

Quattrocchio, M.E., Olivera, D.E., Martínez, M.A., Ponce, J.J. and Carmona, N.B. 2018. Palynofacies associated to hyperpycnite deposits of the Miocene, Cabo Viamonte Beds, Austral Basin, Argentina. Facies 64: 22.

Robbiano, J.A., Arbe, H.A. and Gangui, A. 1996. Cuenca Austral Marina. In: Ramos, V.A. and Turic, M.A. (eds.), Geología y Recursos Naturales de la Plataforma Continental Argentina, Relatorio del 13° Congreso Geológico Argentino y 3° Congreso de Exploración de Hidrocarburos. Asociación Geológica Argentina. Instituto Argentino del Petróleo: 323–341. Buenos Aires.

Romans, B.W., Fildani, A., Hubbard, S.M., Covault, J.A., Fosdick, J.C. and Graham, S.A. 2011. Evolution of deep-water stratigraphic architecture, Magallanes Basin, Chile. Marine and Petroleum Geology 28: 612-628.

Sachse, V.F., Strozyk, F., Anka, Z., Rodriguez, J.F. and di Primio, R. 2015. The tectonostratigraphic evolution of the Austral Basin and adjacent areas against the background of Andean tectonics, southern Argentina, South America. Basin Research 28(4): 462-482.

Schwarz, E. and Arnott, R.W.C. 2007. Anatomy and evolution of a slope channel complex set (Neoproterozoic Isaac Formation, Windermere Supergroup, southern Canadian Cordillera): implications for reservoir characterization: Journal of Sedimentary Research 77: 89-109.

Tassone, A., Lodolo, E., Menichetti, M., Yagupsky, D., Caffau, M. and Vilas, J. 2008. Seismostratigraphic and structural setting of the Malvinas Basin and its southern margin (Tierra del Fuego Atlantic offshore). Geologica Acta 6: 55-67.

Torres Carbonell, P.J. 2010. Control tectónico en la estratigrafía y sedimentología de secuencias sinorogénicas del Cretácico Superior-Paleógeno de la faja corrida y plegada Fueguina. Doctoral tesis, Universidad Nacional del Sur (unpublished), 384 p., Bahía Blanca.

Torres Carbonell, P.J. and Olivero, E.B. 2012. Sand dispersal in the southeastern Austral Basin, Tierra del Fuego, Argentina: outcrop insights from Eocene channeled turbidite systems. Journal of South American Earth Sciences 33: 80-101.

Torres Carbonell, P.J. and Olivero, E.B. 2019. Tectonic control on the evolution of depositional systems in a fossil, marine foreland basin: Example from the SE Austral Basin, Tierra del Fuego, Argentina. Marine and Petroleum Geology 104: 40-60.

Torres Carbonell, P.J., Dimieri, L.V. and Olivero, E.B. 2011. Progressive deformation of a Coulomb thrust wedge: the eastern Fuegian Andes thrust-fold belt. In: Poblet, J. and Lisle, R. (eds.), Kinematic Evolution and Structural Styles of Fold-And-Thrust Belts. Geological Society, London, Special Publications. The Geological Society 349: 123-147.

Torres Carbonell, P.J., Dimieri, L.V. and Martinioni, D.R. 2013. Early foreland deformation of the Fuegian Andes (Argentina): constraints from the strain analysis of Upper Cretaceous-Danian sedimentary rocks. Journal of Structural Geology 48: 14-32.

Torres Carbonell, P.J., Dimieri, L.V., Olivero, E.B., Bohoyo, F. and Galindo-Zaldivar, J. 2014. Structure and tectonic evolution of the Fuegian Andes (southernmost south America) in the framework of the scotia arc development. Global and Planetary Change 123 (Part B): 174-188.

Torres Carbonell, P.J., Cao, S.J. and Dimieri, L.V. 2017a. Spatial and temporal characterization of progressive deformation during orogenic growth: example from the Fuegian Andes, southern Argentina. Journal of Structural Geology 99: 1-19.

Torres Carbonell, P.J., Rodriguez Arias, L., Atencio, M.R. 2017b. Geometry and kinematics of the Fuegian thrust-fold belt, southernmost Andes. Tectonics 36: 33-50.

Torres Carbonell, P.J., Cao, S.J., González Guillot, M., Mosqueira González, V.M., Dimieri, L.V., Duval, F. and Scaillet, S. 2020. The Fuegian thrust-fold belt: From arc-continent collision to thrust-related deformation in the southernmost Andes. Journal of South American Earth Sciences 102: 102678.